Zero Emissions Research and Technology (ZERT) II – Investigating the Fundamental Scientific Issues Affecting the Long-term Geologic Storage of Carbon Dioxide

Project Number DE-FE0000397

Lee H Spangler

Energy Research Institute

Montana State University

U.S. Department of Energy

National Energy Technology Laboratory
Carbon Storage R&D Project Review Meeting
Developing the Technologies and Building the Infrastructure for CO_2 Storage

August 21-23, 2012

Presentation Outline

- Computational tool development
- Laboratory studies to understand subsurface CO_2 behavior
- Analog studies to inform risk analysis
- Near surface detection technologies / testing
- Mitigation method development

Benefit to the Program

Program goals being addressed.

- Develop technologies that will support industries' ability to predict CO_2 storage capacity in geologic formations to within ±30 percent.
- Develop technologies to demonstrate that 99 percent of injected CO_2 remains in the injection zones.
- Conduct field tests through 2030 to support the development of BPMs for site selection, characterization, site operations, and closure practices.

Project benefits statement.

ZERT II supports Storage Program goals by 1) developing computational tools for simulating CO_2 injection, storage and trapping, 2) performing basic geoscience experiments to address relationships between properties such as wetting, relative permeability, saturation, and capillary pressure that will improve understanding of CO_2 behavior in the reservoir and help with model parameterization 3) investigating analogs to understand risks to storage security 4) conducting field experiments to test near surface monitoring technologies and 5) developing novel bio-controlled leakage mitigation technology

Project Overview:
Goals and Objectives

Biofilms and Biomineralization

- Objective: Perform a comprehensive evaluation of techniques for current and novel CO_2 sequestration concepts associated with microbial biofilms.

Natural Analogs of Escape Mechanisms

- Objective: Characterize the physical, mineralogical, and geochemical characteristics of a fracture system that may have been exposed to naturally occurring sub-surface CO_2, for the purpose of determining the reservoir and trap conditions that contribute to long-term CO_2 sequestration versus those that contribute to CO_2 leakage.
- Objective: Characterize the physical, mineralogical, and geochemical characteristics of outcrops of hydrothermal plume related rocks to determine their usefulness as natural analogs of breached and healed caprocks for carbon sequestration.

Optical Detection for Carbon Sequestration Site Monitoring

- Objective: Demonstrate the feasibility of creating an in-line fiber optic sensor for CO_2 that utilizes sections of photonic bandgap (PBG) fibers interspersed with sections of single mode optical fiber.
- Objective: Develop a custom-designed multispectral imager to detect CO_2 -induced plant stress with lower cost to allow field deployment of multiple imagers for monitoring large, distributed carbon sequestration facilities.

Validation of Near-surface CO_2 Detection Techniques and Transport Models

- Objective: Determine, via field experimentation, the efficacy and detection limits for existing and emerging near-surface CO_2 detection technologies.

Project Overview: Goals and Objectives

Task 2.0 – Biofilms and Biomineralization

- Decision Point – Results of pulsed flow experiments concerning ability to control deposition rate and spatial distribution of biofilm barriers.
- Success Criteria – Ability to provide a spatial distribution over an area greater than one inch from in-flow side of porous media.

Task 3.0 – Natural Analogs of Escape Mechanisms

- Decision Point – The geologic outcrop studies must produce enough data to make time investment of development of a three-dimensional static model.
- Success Criteria – One hydrothermal plume of sufficient detail has already been identified, so success is highly probable. The key issue here is determining which plume provides the most appropriate information. We will discuss this with other geoscientists and modelers to make this determination.

Task 4.0 – Optical Detection for Carbon Sequestration Site Monitoring

- Decision Point – Demonstration of the ability to re-launch light into subsequent fiber sections when an air gap is left between the sections.
- Success Criteria – Ability to re-launch and propagate light on the subsequent fiber section. If this is not possible, a different method of sampling the soil gas via fiber will likely be necessary.
- Decision Point – Multispectral imager prototype field test results
- Success Criteria – Spatial resolution and spectral performance will be tested and NDVI or other image processing will be compared to commercial instruments.

Task 5.0 – Validation of Near-surface CO_2 Detection Techniques and Transport Models

- Decision Point – Many personnel – hours are spent by multiple institutions in the field experiment. Successful preparation / re-installation of field infrastructure must occur before conducting field experiment.
- Success Criteria – Packer system must inflate and hold pressure, mass flow control system must be functioning.

Technical Status

- Focus the remaining slides, logically walking through the project. Focus on telling the story of your project and highlighting the key points as described in the Presentation Guidelines
- When providing graphs or a table of results from testing or systems analyses, also indicate the baseline or targets that need to be met in order to achieve the project and program goals.

TOUGHREACT Version 2.0

Computers & Geosciences 37 (2011) 763–774

Contents lists available at ScienceDirect

Computers & Geosciences

journal homepage: www.elsevier.com/locate/cageo

ELSEVIER

TOUGHREACT Version 2.0: A simulator for subsurface reactive transport under non-isothermal multiphase flow conditions

Tianfu Xu *, Nicolas Spycher, Eric Sonnenthal, Guoxiang Zhang [1], Liange Zheng, Karsten Pruess

Earth Sciences Division, Lawrence Berkeley National Laboratory, 1 Cyclotron Road, Berkeley, CA 94720, USA

A R T I C L E I N F O

Article history:
Received 12 April 2010
Received in revised form
17 August 2010
Accepted 5 October 2010
Available online 18 November 2010

Keywords:
Multi-phase flow
Reactive transport
TOUGHREACT
CO_2 geological storage
Environmental remediation
Nuclear waste geological disposal

A B S T R A C T

TOUGHREACT is a numerical simulation program for chemically reactive non-isothermal flows of multiphase fluids in porous and fractured media, and was developed by introducing reactive chemistry into the multiphase fluid and heat flow simulator TOUGH2 V2. The first version of TOUGHREACT was released to the public through the U.S. Department of Energy's Energy Science and Technology Software Center (ESTSC) in August 2004. It is among the most frequently requested of ESTSC's codes. The code has been widely used for studies in CO_2 geological sequestration, nuclear waste isolation, geothermal energy development, environmental remediation, and increasingly for petroleum applications. Over the past several years, many new capabilities have been developed, which were incorporated into Version 2 of TOUGHREACT. Major additions and improvements in Version 2 are discussed here, and two application examples are presented: (1) long-term fate of injected CO_2 in a storage reservoir and (2) biogeochemical cycling of metals in mining-impacted lake sediments.

TOUGH2/EOS7CA

	Soil
Temperature (T)	15 ^oC
Porosity (ϕ)	0.30
Permeability (k)	1 x 10^{-12} m^2
Capillary Pressure (P_c)	van Genuchten[1,2] $\lambda = 0.2$, $S_{lr} = 0.11$, $\alpha = 8.5$ x 10^{-4} Pa^{-1}, $P_{max} = 1$ x 10^{10} Pa, $S_{ls} = 1$.
Relative permeability (k_r)	van Genuchten[1,2] $S_{lr} = 0.10$, $S_{gr} = 0.01$
Molec. diffusivity coefficients (d_β^κ)	Liquid: 10^{-10} m^2 s^{-1} Gas: 10^{-5} m^2 s^{-1} $\theta = 1.0$, $P_0 = 10^5$ Pa
Tortuosity (τ_0)	1.0
Saturation-dependent tortuosity (τ_β)	Equal to relative permeability

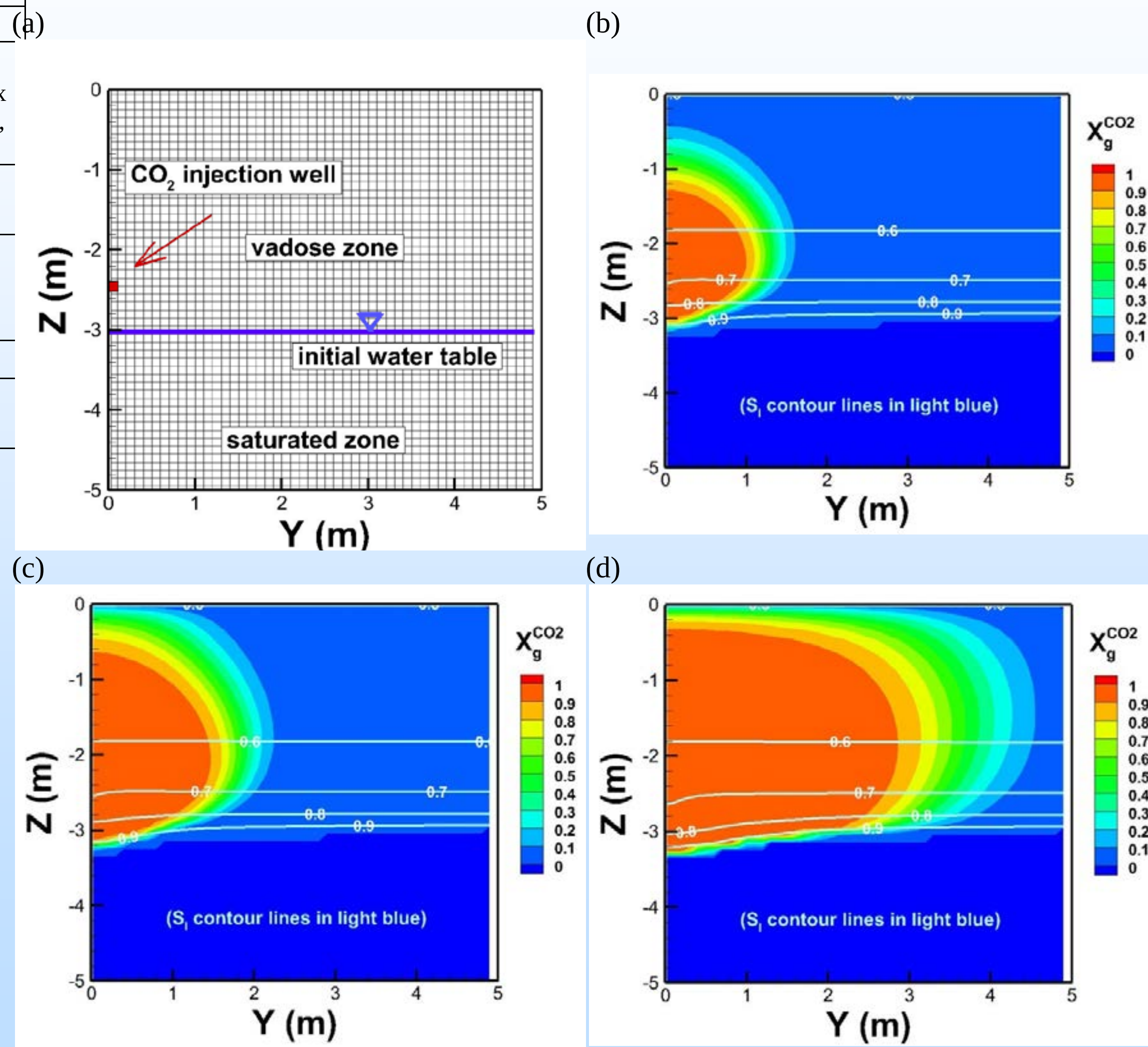

EOS7CA uses a cubic equation of state with a multiphase version of Darcy's Law to model flow and transport of gas and aqueous phase mixtures (water, brine, NCG, gas tracer, air, and optional heat) over a range of pressures and temperatures appropriate to shallow subsurface porous media systems.

Development of numerical models for simulating coupled fluid-flow and stress effects

- Geomechanical impacts of large-scale injection during CO_2 storage operations is one of the critical issues in ensuring safe operations and long-term reliability of geologic CO_2 sequestration sites
- We have developed capabilities in LANL's FEHM reservoir simulator to model complex, coupled non-isothermal, multi-phase flow and geomechanical processes:
  - Non-linear elasticity: elastic moduli as functions of temperature, pressure, and stress
  - Stress-dependant permeability models : Non-linear, orders-of-magnitude permeability changes, explicitly or Implicitly coupled .
  - Wellbore cement failure: interface evolution due to geomechanical effects
  - Plastic deformation

Los Alamos

Examples demonstrating new, complex fluid-flow and stress modeling capabilities in FEHM

Simulation of change in the permeability in a fault due to injection in a nearby wellbore

Permeability as a function of change in normal stress

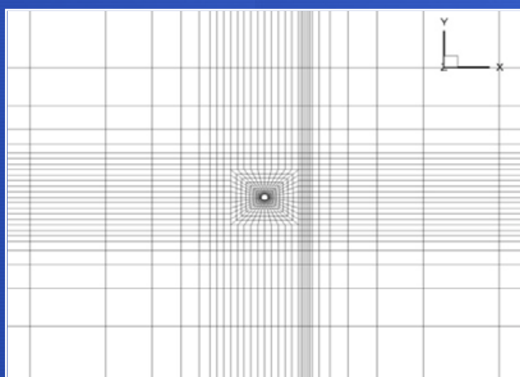

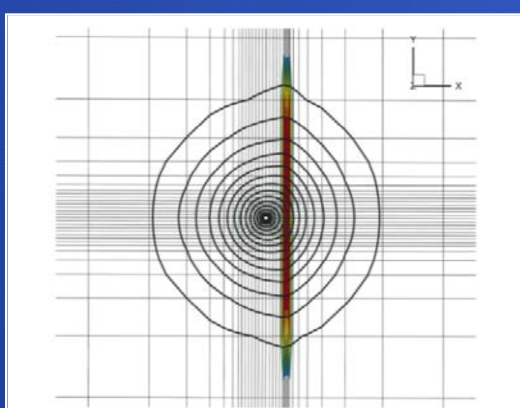

Simulation of change in permeability in an inclined fault due to injection

- Non-orthogonal grid
- Thermal effects
- Mohr-Coulomb failure
- Permeability as a function of shear stress

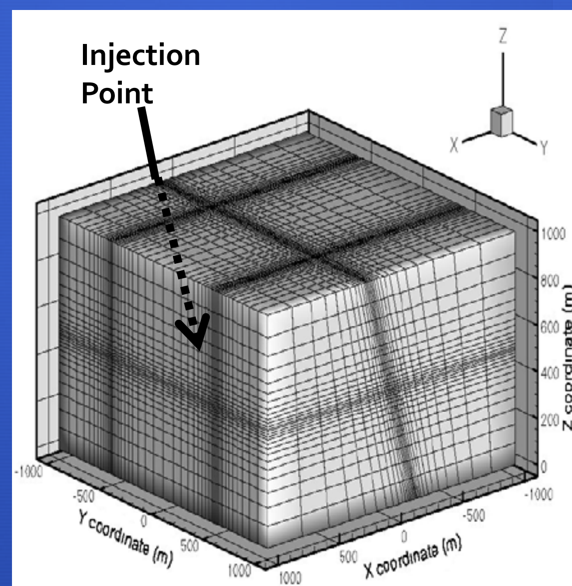

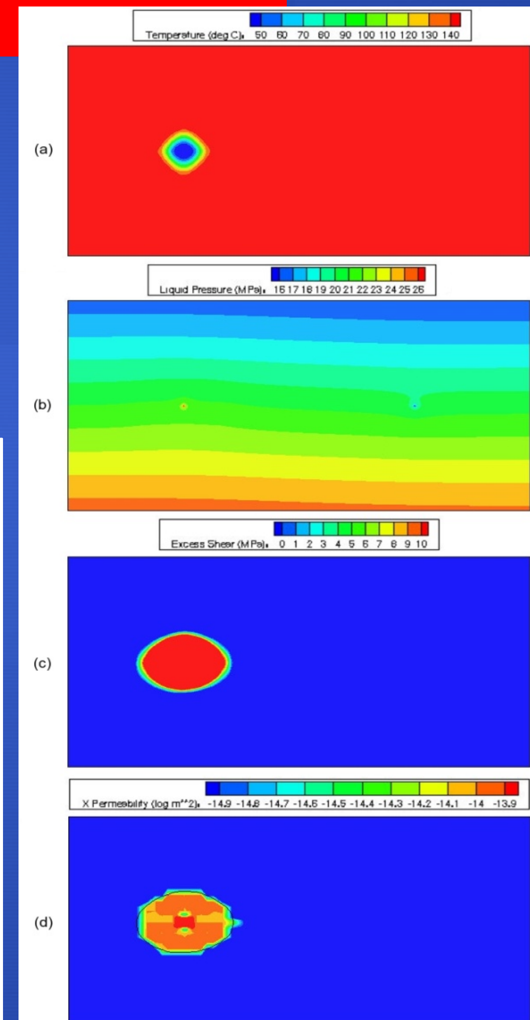

Los Alamos

Comparison of silica/calcite wettability in the brine-$scCO_2$ and brine-N_2 systems

(Tim Kneafsey, Dmitriy Silin)

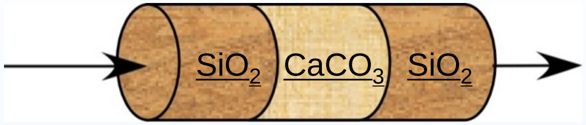

Objective

- Visualize/analyze wettability differences between coarse silica and fine calcite sand in $scCO_2$-brine system

Approach

- Flow N_2 (for comparison) and $scCO_2$ through fine, brine-saturated sands
- Flow brine through sample after N_2, then $scCO_2$ until breakthrough (residual saturation)
- Monitor with X-ray computed tomography (CT)
- Image sand samples with microCT
- Apply Maximal Inscribed Spheres (MIS) model to compute characteristic curves
- Compare to experimental results

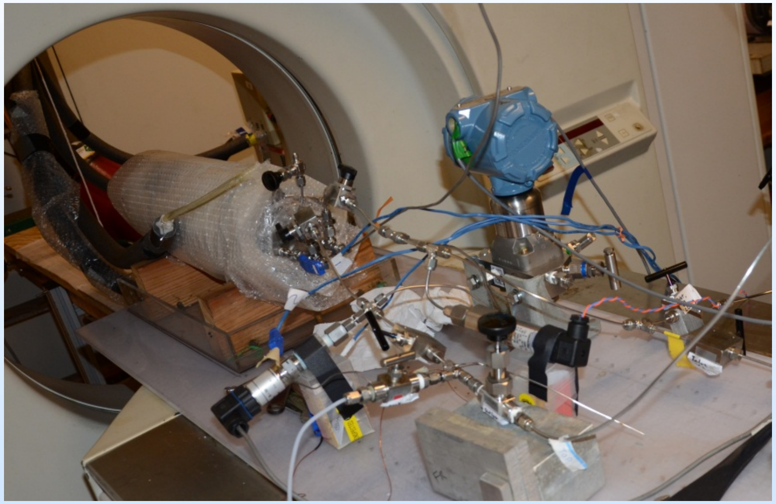

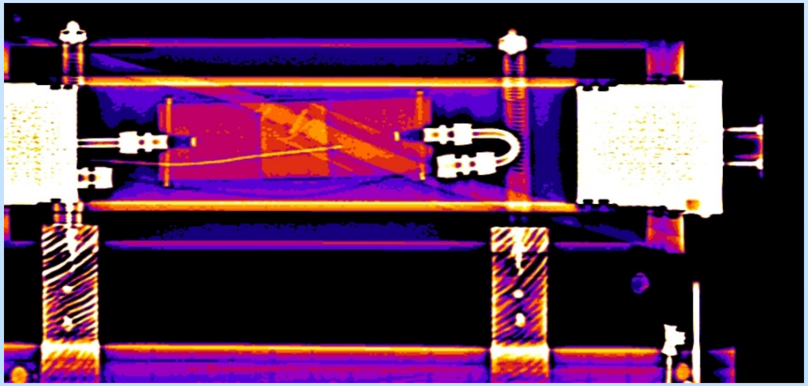

Experimental and Modeling Results

CT images of $scCO_2$ saturation in slices through composite domain (silica-calcite-silica) (calcite section is outlined by white line)

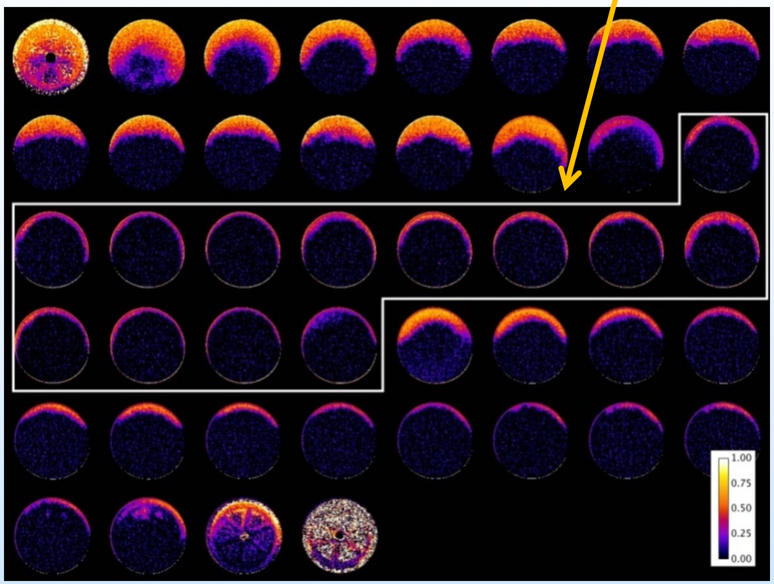

MicroCT imaged sand and calculated pore occupancy by MIS

Computed $scCO_2$ saturation using MIS computations for 0 and 20 degree contact angles

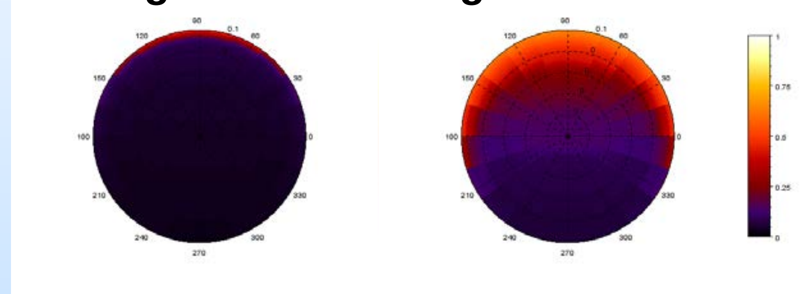

- Both N_2 and CO_2 flowed across sample top due to gravity
- Both N_2 and CO_2 flowed through a larger region of silica than calcite
- Neither N_2 or CO_2 penetrated deeply into calcite indicating strongly brine-wetting conditions

- Computations based on the MIS technique including contact angle indicate that both silica and calcite are brine-wetting, but calcite is strongly brine-wetting under the experiment conditions.

Capillary Pressure-Saturation Relations

(Jiamin Wan and Tetsu Tokunaga)

- Saturation-capillary pressure, $S(P_c)$, relations are needed to determine equilibrium of CO_2-brine, relative permeability relations, flow, and residual trapping of CO_2.

- Measurements are being done on well-characterized, uniform sands in order to quantitatively compare results with predictions based on capillary scaling models.

- Our experimental system is capable of measuring $S(P_c)$ relations on unconsolidated (sands) and consolidated (cores).

- Experiments have been conducted on air-water systems at atmospheric pressure and 20˚C, and on $scCO_2$-water(brine) systems at high pressure (8.5 to 12 MPa) and 45˚C.

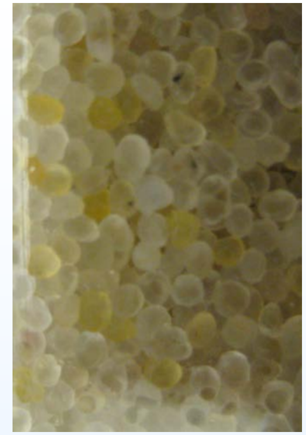

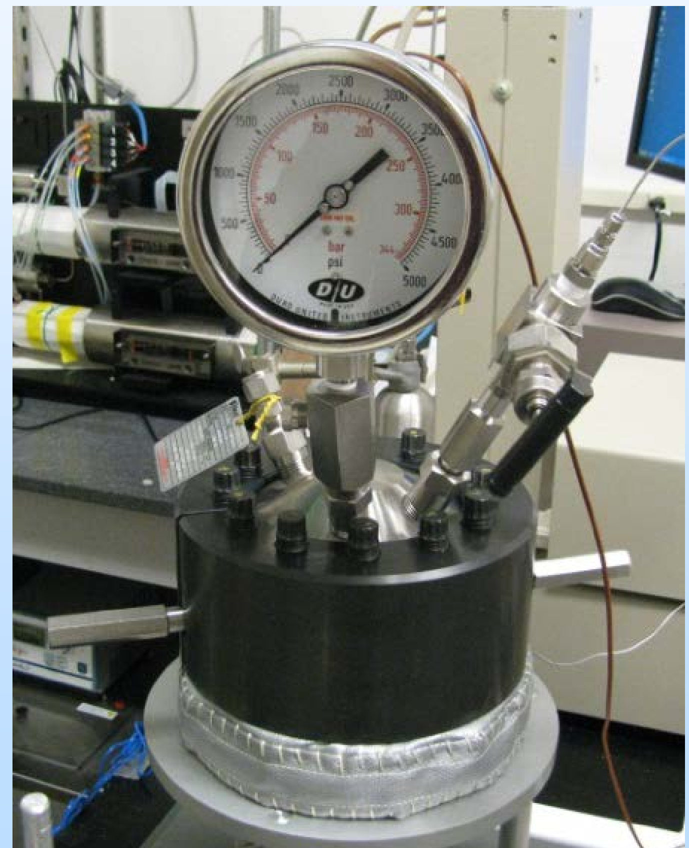

P_c dependence on brine (1 M NaCl) phase water content

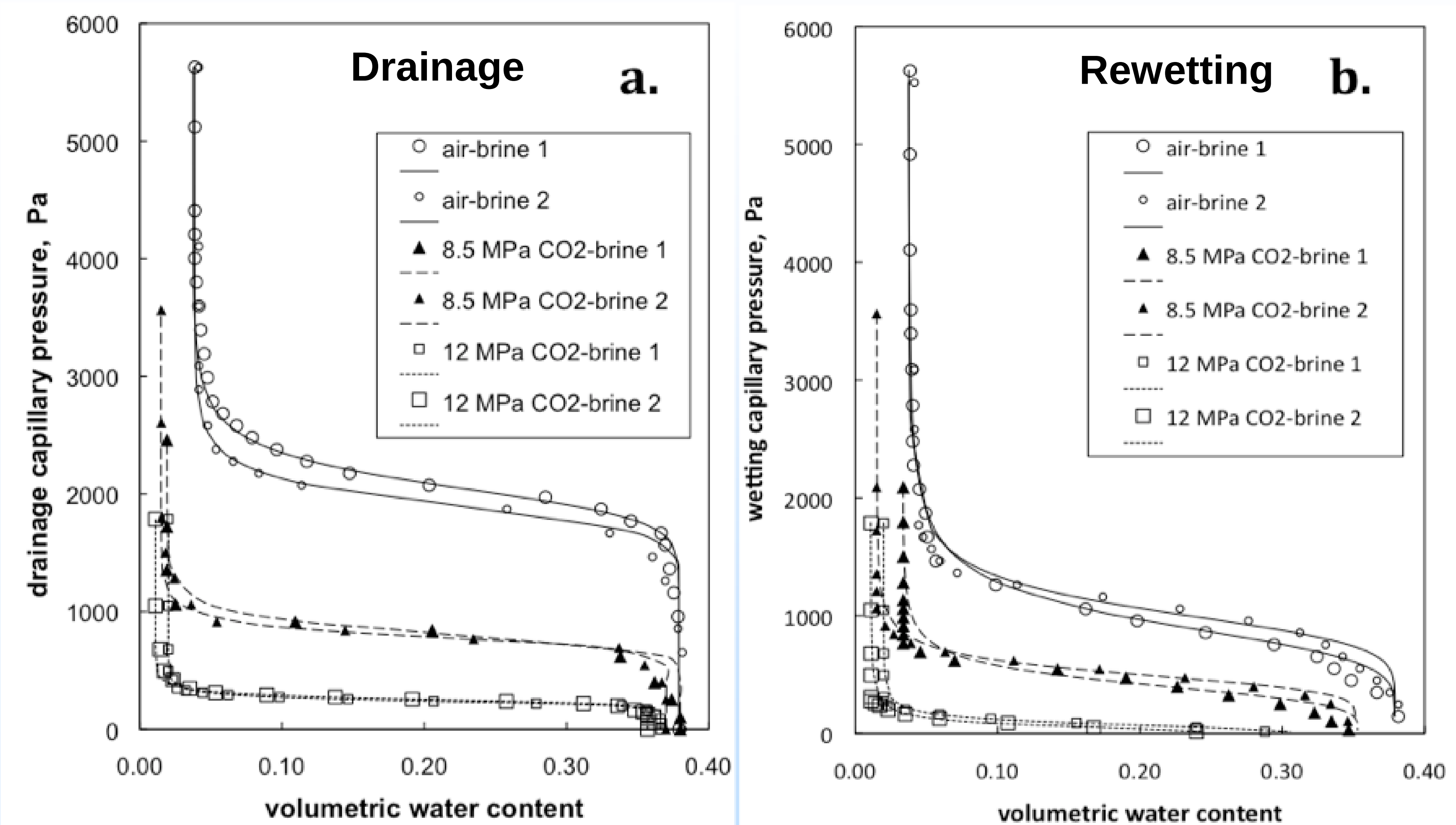

Capillary (residual) trapping of $scCO_2$ is higher relative to air as the nonwetting phase. Higher residual trapping of $scCO_2$ is achieved at higher total P

NMR Imaging

Limestone Sandstone

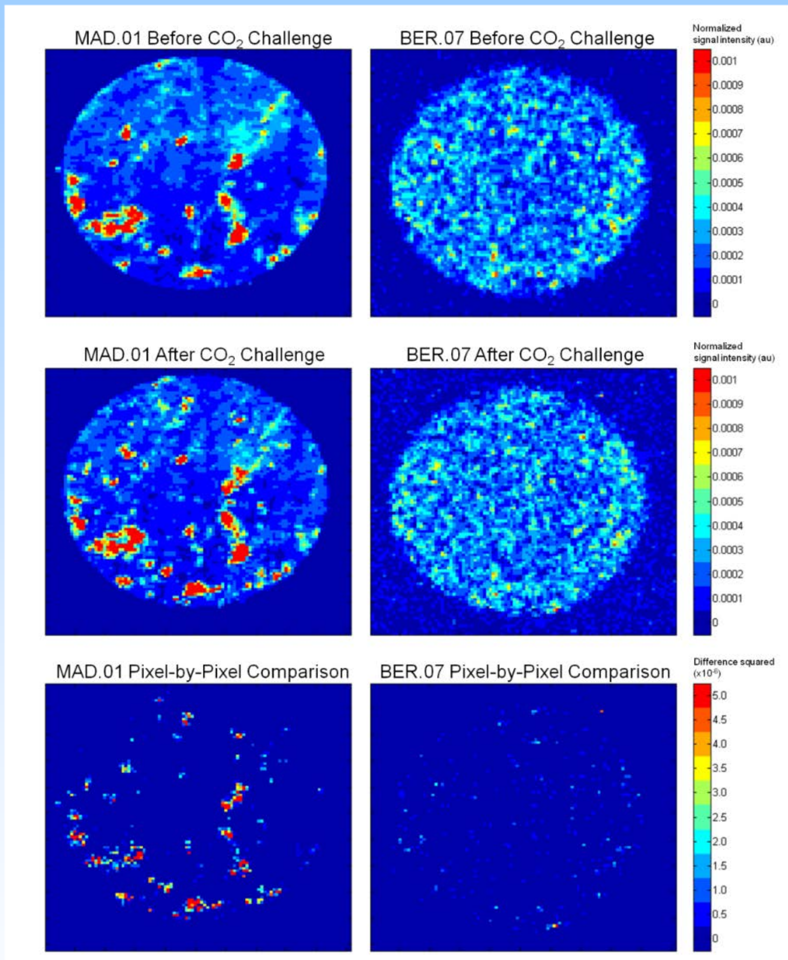

Limestone

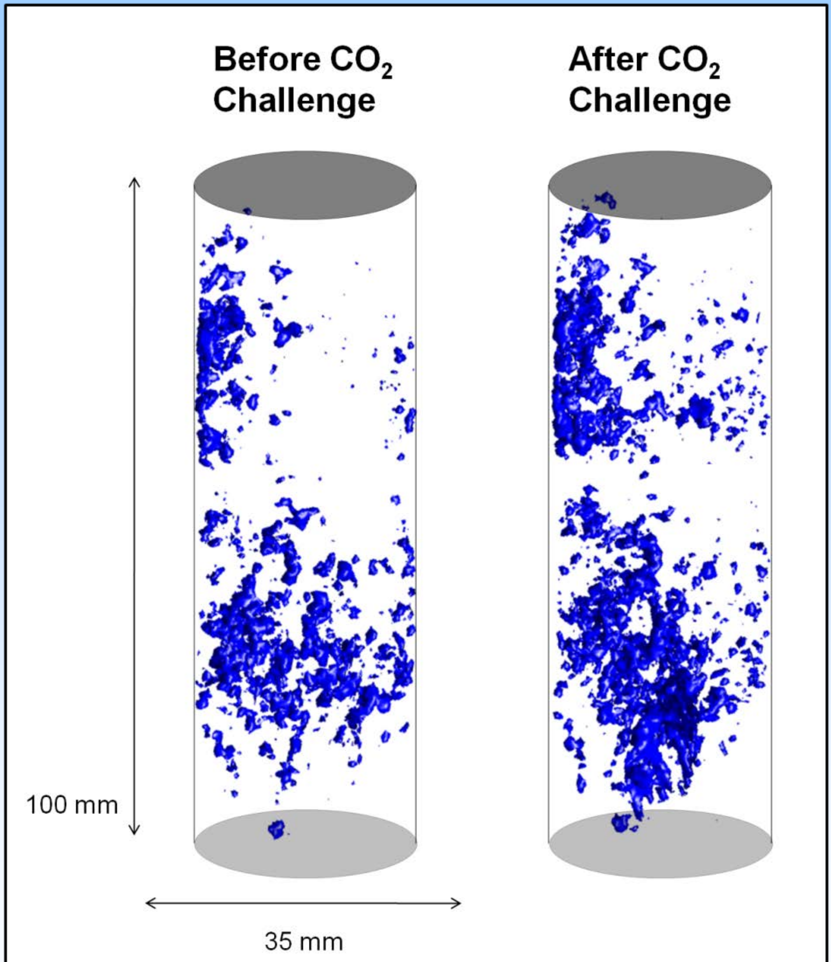

C. A. Shaw, S. J. Vogt, J. E. Maneval, T. Brox, M. L. Skidmore, S. L. Codd, J. D. Seymour

ZERT Zero Emissions Research and Technology

MONTANA STATE UNIVERSITY

T_2-T_2 Before and After CO_2 Challenge

Madison Limestone Before Challenge

Madison Limestone After Challenge

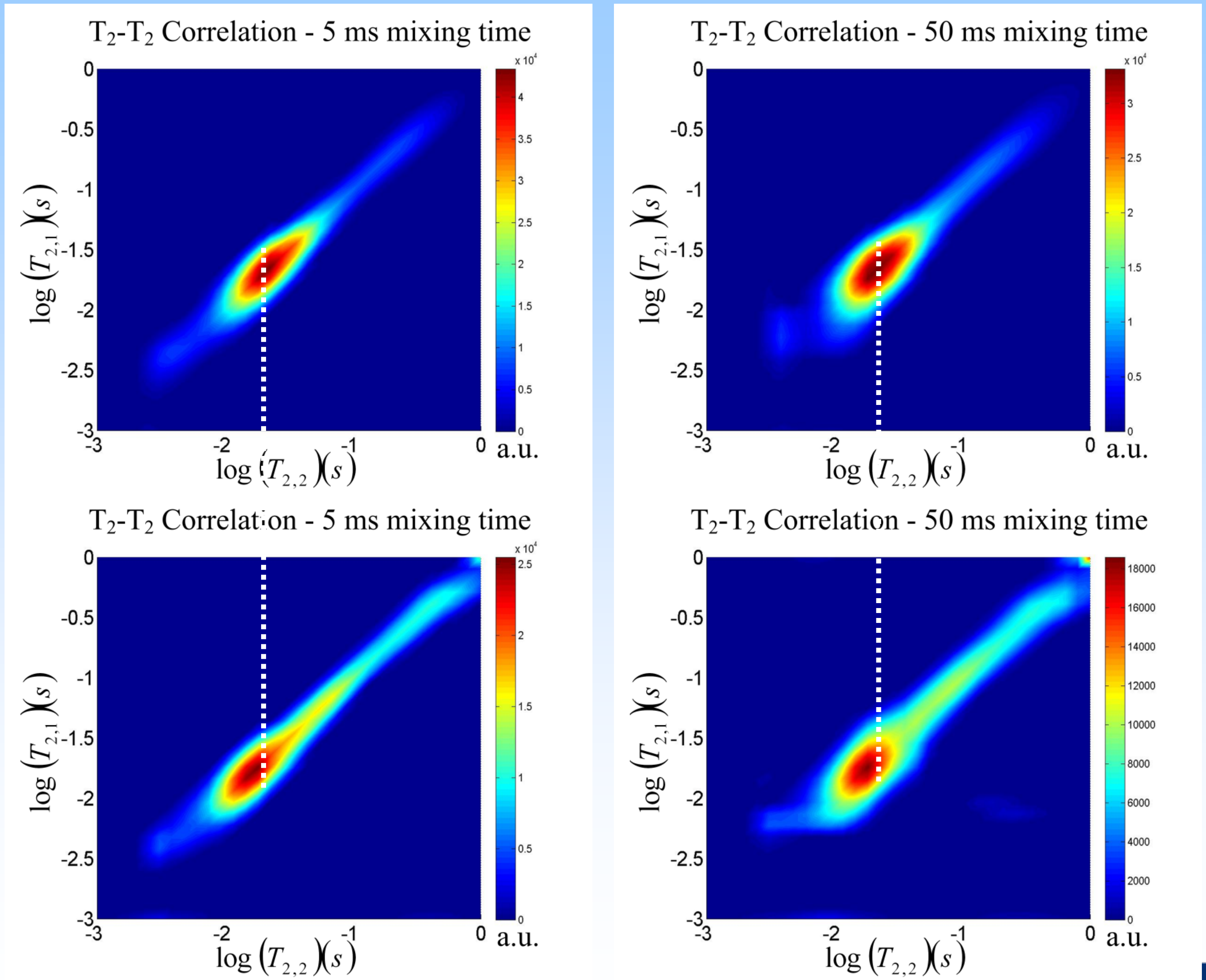

T_2-T_2 Before and After CO_2 Challenge

Berea Sandstone Before Challenge

Berea Sandstone After Challenge

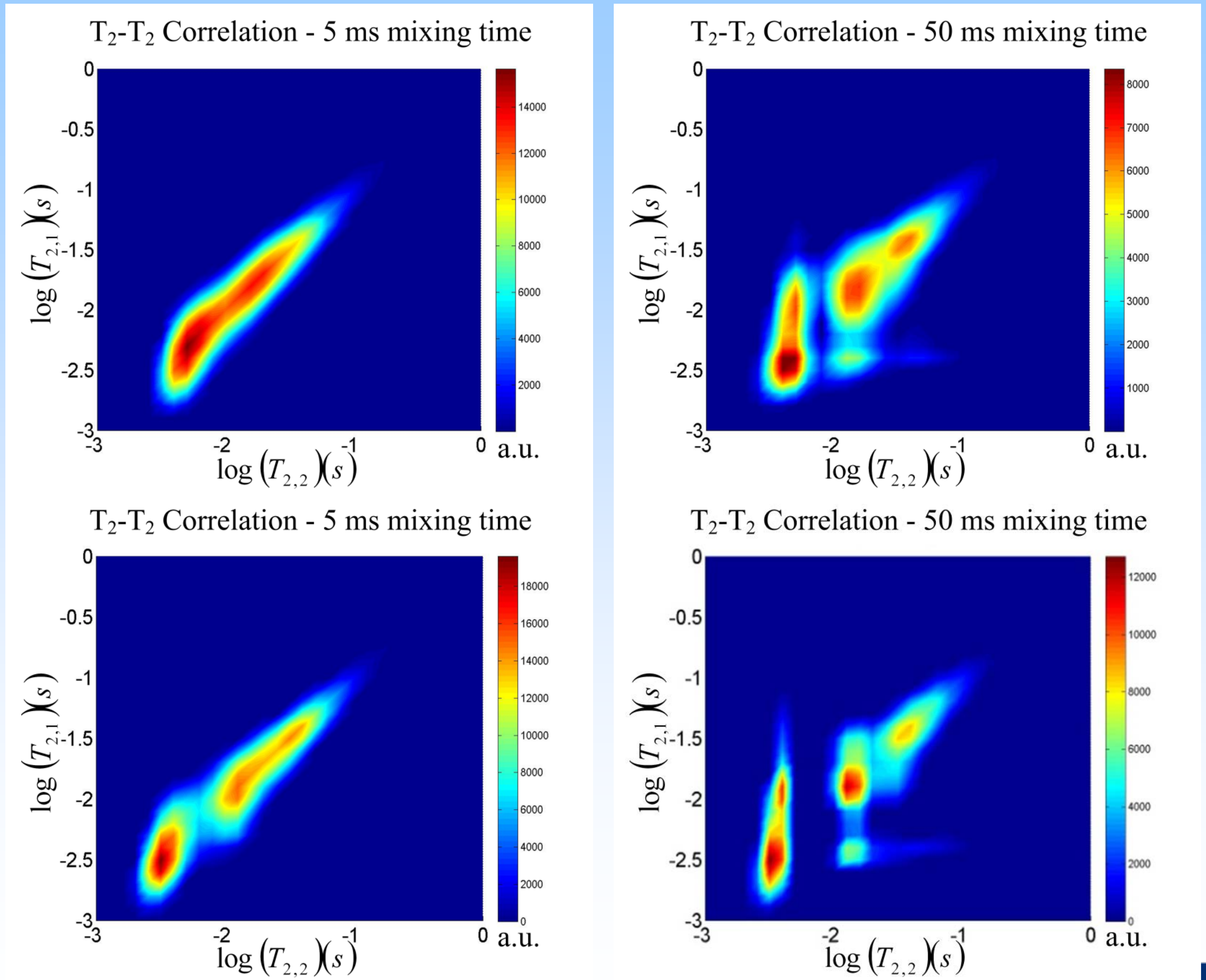

ZERT Zero Emissions Research and Technology

MONTANA STATE UNIVERSITY

Core Holder for in-situ MRI Studies

Core Holder Schematic

A. Core-challenge fluid (outlet)
B. Recirculating fluid (outlet)
C. Recirculating fluid (inlet)
D. Core-challenge fluid (inlet)
E. Thermocouple
F. PEEK composite sheath

Max. pressure: 5000 psi
Max. temperature: 150°C

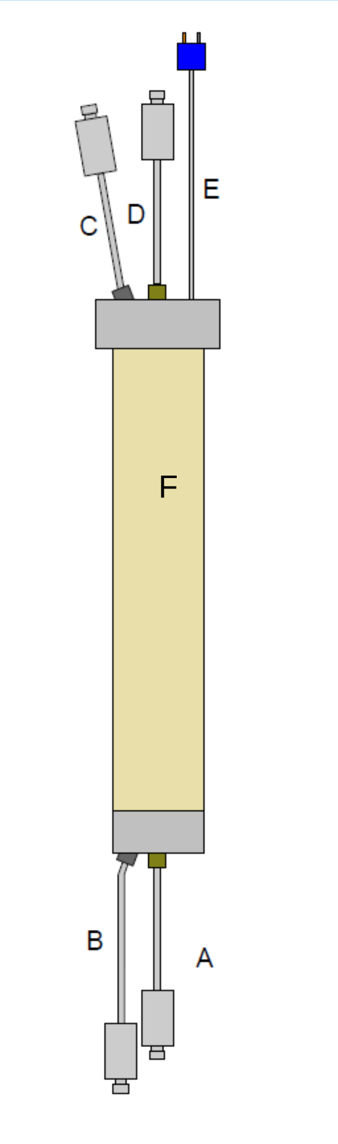

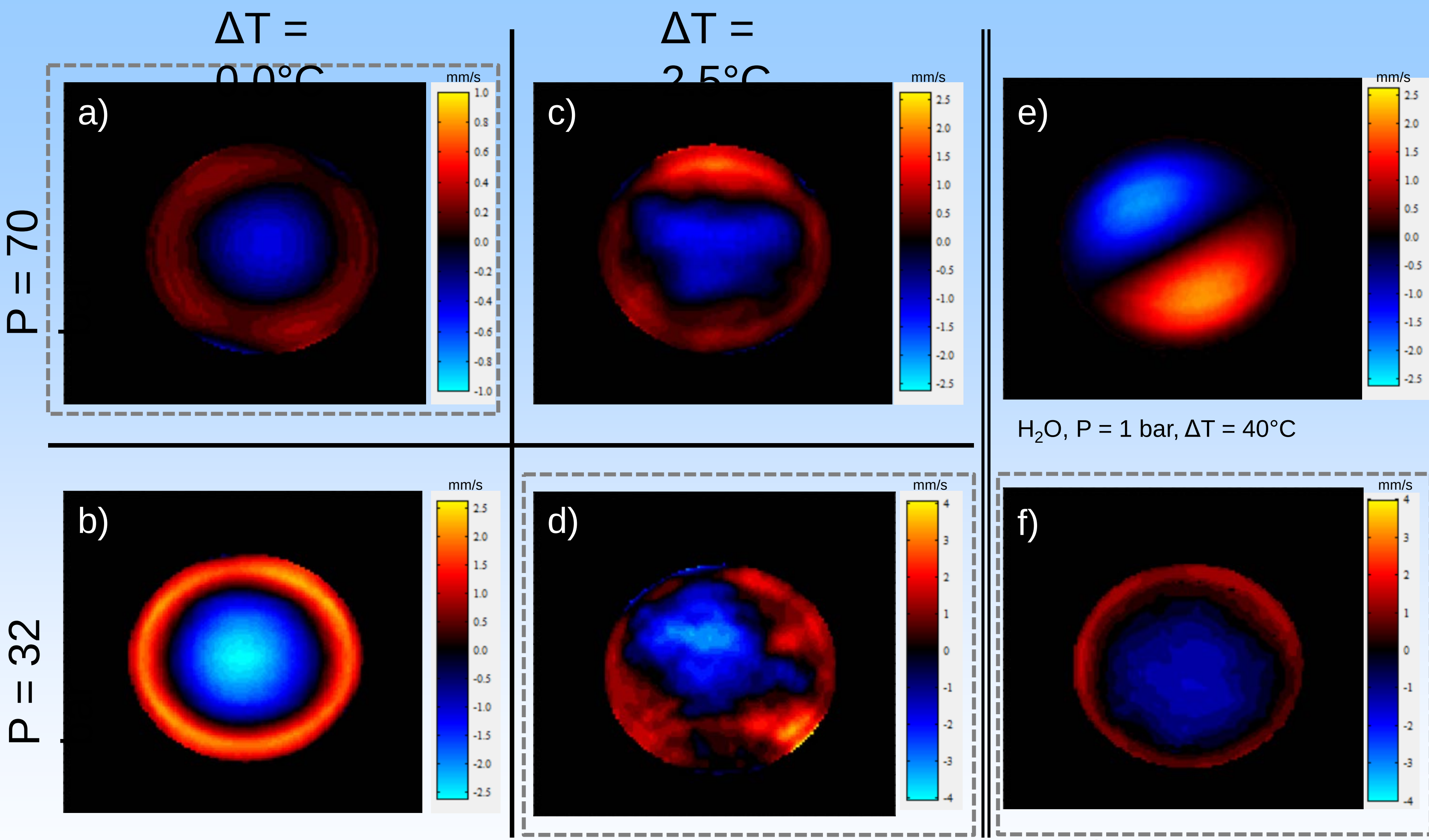

Axial velocity maps for supercritical C_2F_6 (a-d,f) and liquid H_2O (e). The "bull's eye" pattern of the C_2F_6 is due to large thermal expansion in the supercritical regime and a wall heat-transfer mechanism. All images averaged over 1 hour, except (f), which was averaged over 11 hours.

Natural Analogs of Escape Mechanisms

Natural Analogs of Escape Mechanisms

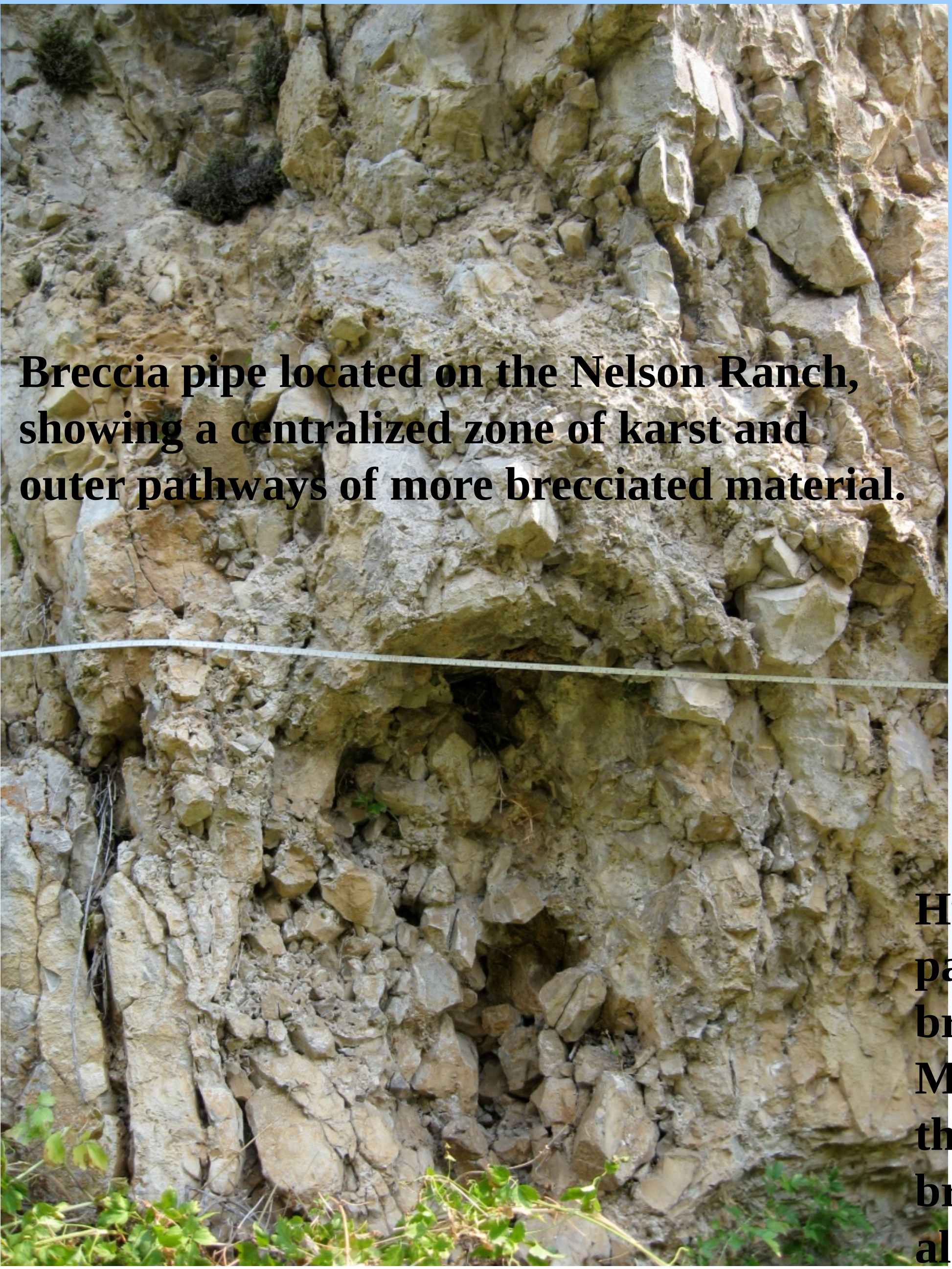

Breccia pipe located on the Nelson Ranch, showing a centralized zone of karst and outer pathways of more brecciated material.

Hydrothermal breccia formed along a strike parallel b-c fracture with a preexisting collapsed breccia. The bottom of the breccia shows Madison Limestone beds being upturned while the top displays collapse features with a chaotic breccia. This site also had dolomite vein fill along some of the adjacent small fractures.

Natural Analogs of Escape Mechanisms

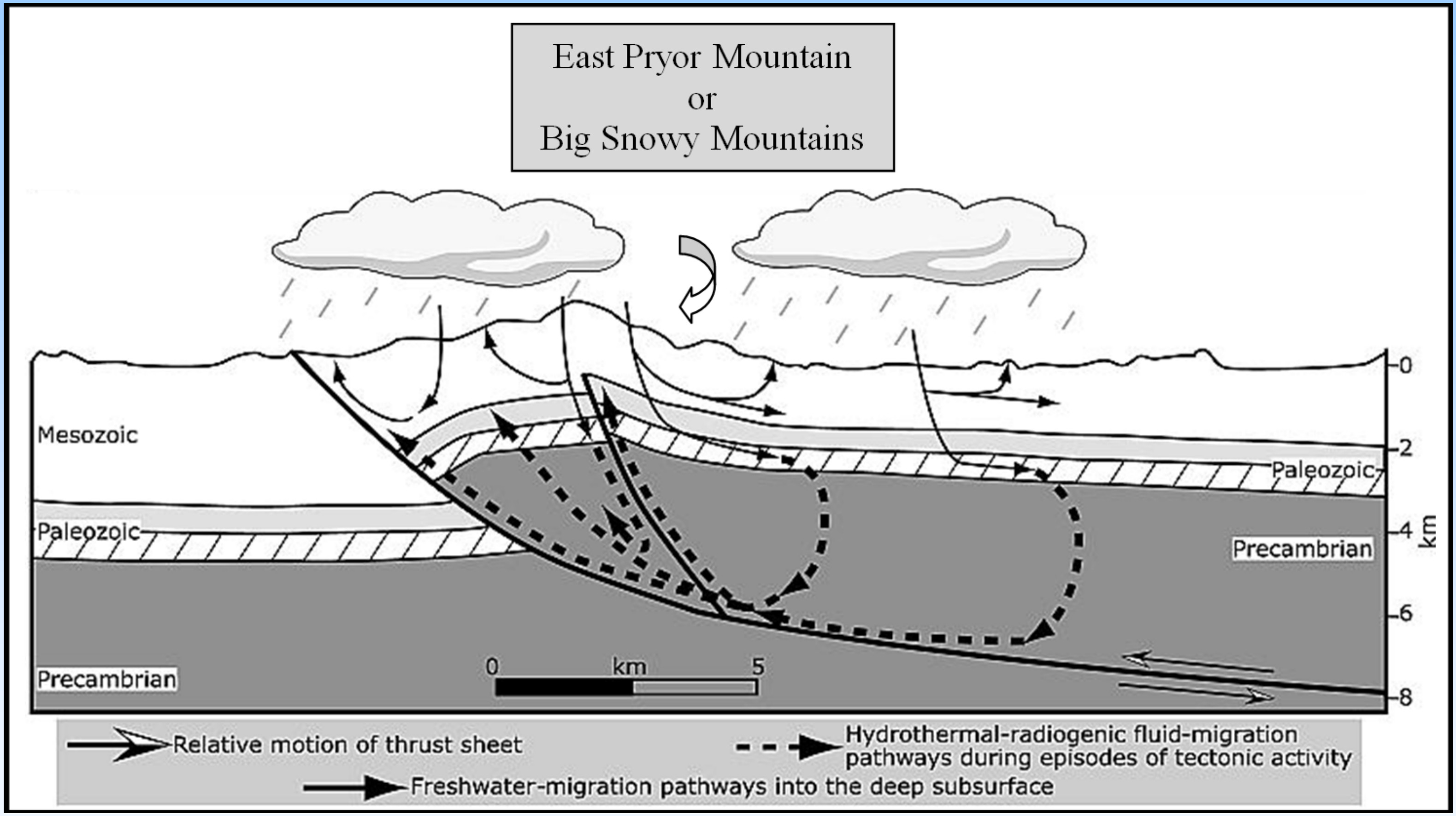

Figure adapted from Katz et al, 2006; Huntoon, 1993, showing model of possible freshwater and hydrothermal fluid-migration pathways along a high-angle basement fault which could account for depleted $\delta^{18}O$ late-stage calcite and dolomite precipitated along brecciated zones and fracture systems in the two study areas.

ZERT Zero Emissions Research and Technology

MONTANA STATE UNIVERSITY

Natural Analogs of Escape Mechanisms

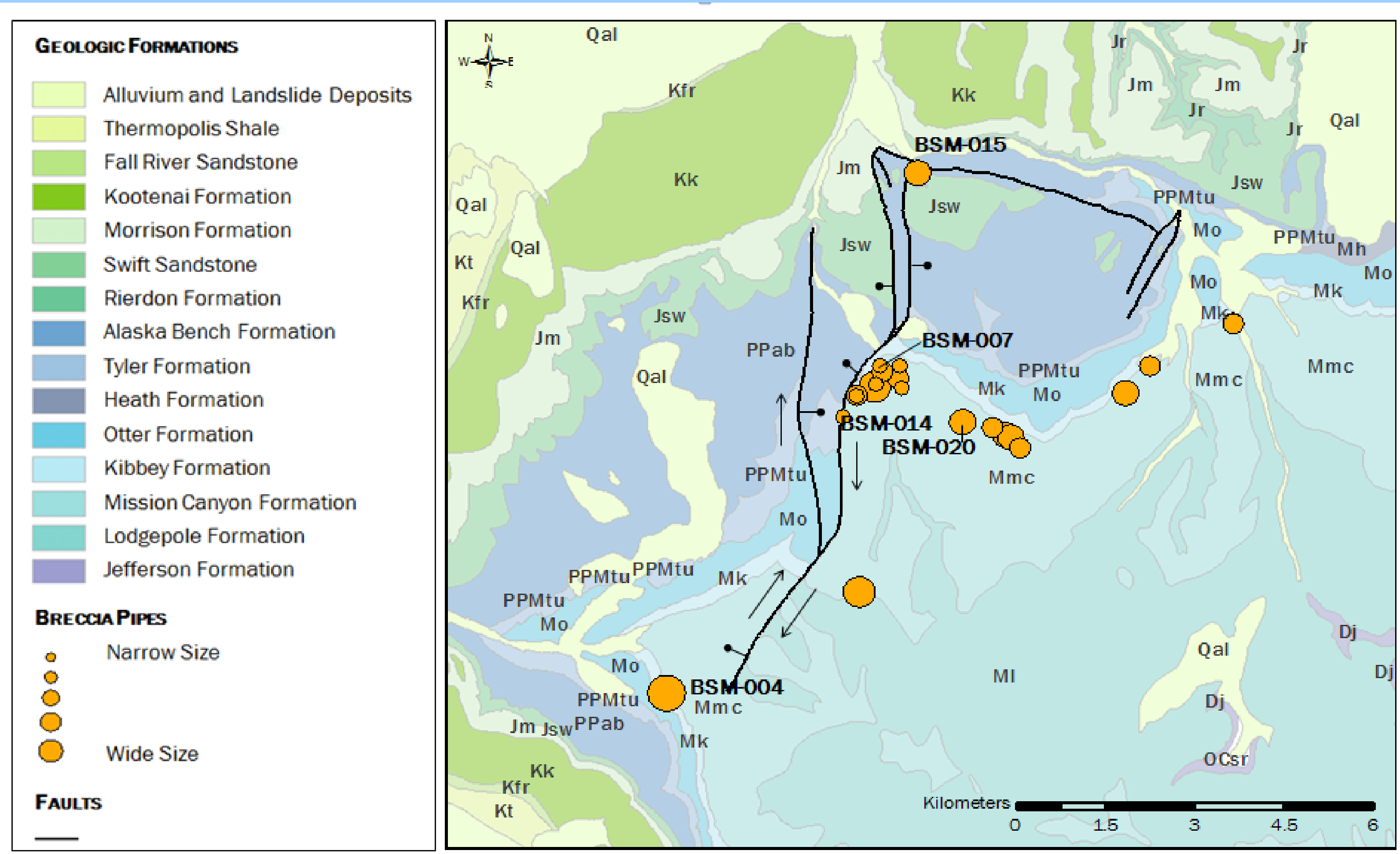

Geologic map of fault/ fracture system in the western Big Snowy Mountains. Breccia pipes are classified based on their width, and range from ~0.5-30 meters. Relative displacement vectors show fault motion. Ball and bar are on down-dropped side of fault.

Zero Emissions Research and Technology

MONTANA STATE UNIVERSITY

Natural Analogs of Escape Mechanisms

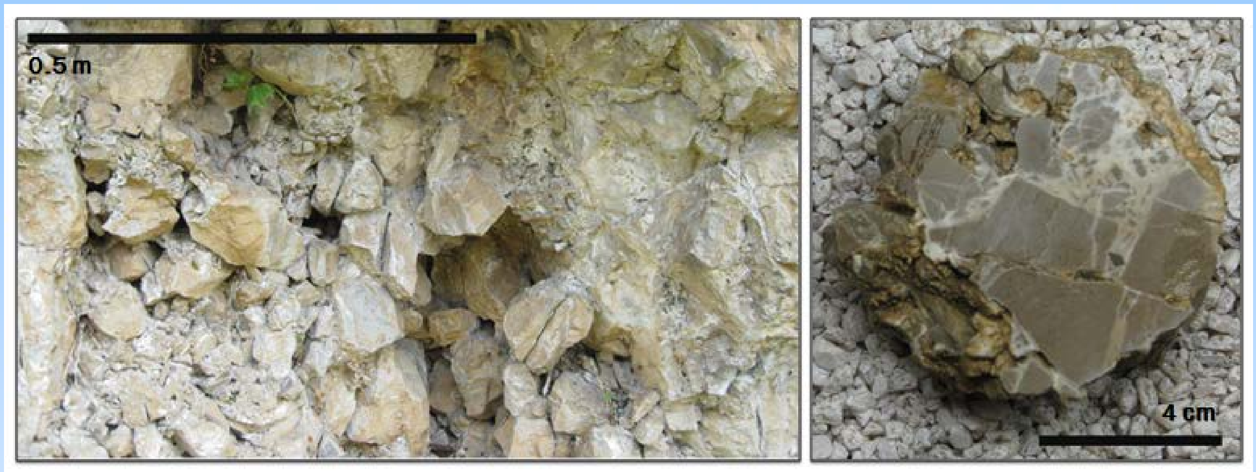

BSM-007: (left) Mission Canyon limestone; field photo of large (up to 23 cm) blocky clasts in central cavity of breccia pipe; very poor sorting; chaotic brecciation. (right) BSM-007b: hand sample of hydrothermal breccia collected from within central cavity of breccia pipe.

BSM-015: (left) Contact between the Alaska Bench Fm. below and the Swift Member of the Ellis Group above. Brecciation is confined to the lower unit. (right) BSM-015b: Hand sample of the breccia.

ZERT Zero Emissions Research and Technology

MONTANA STATE UNIVERSITY

Natural Analogs of Escape Mechanisms

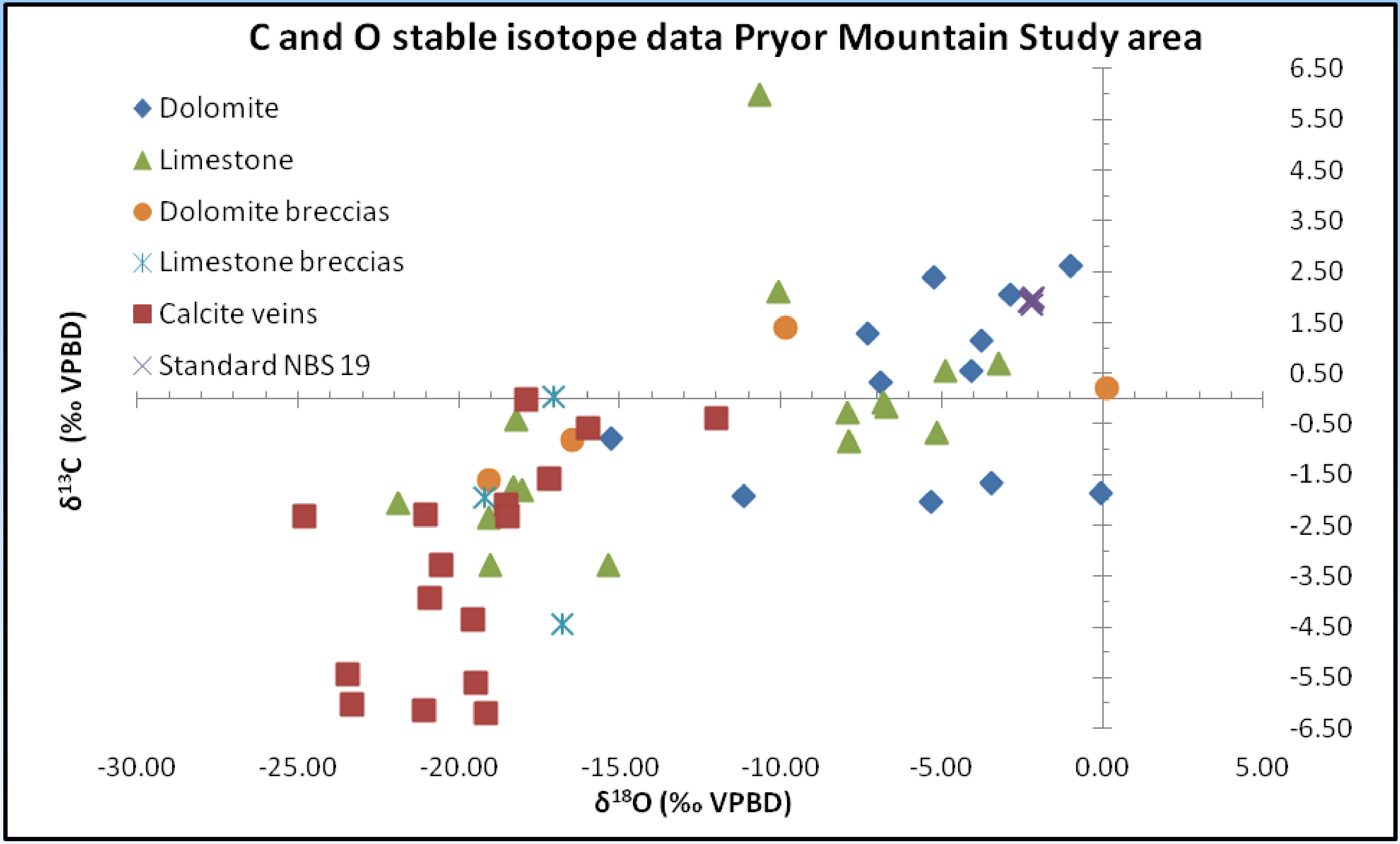

Stable carbon and oxygen isotope analyses of dolomite, limestone, breccias and calcite vein fill material from the Pryor Mountain study area. Red symbols reflect the most depleted $\delta^{18}O$ and $\delta^{13}C$ values in calcite vein material associated with the breccias and fractures in the area. Most of the breccia samples also reflect depleted isotope values relative to standard VPBD. The NBS 19 standard is from University of Michigan Stable Isotope Laboratory.

ZERT Zero Emissions Research and Technology

MONTANA STATE UNIVERSITY

Natural Analogs of Escape Mechanisms

The following conclusions can be made about potential CO_2 reservoir rocks:

1. Hydrothermal alteration follows pre-existing faults, fractures, and joints that are aligned with the regional stress field at the time of formation. Such brittle features often follow A/C and B/C joints in relation to fold geometry. Hydrothermal breccia pipes, which form in conjunction with this alteration, are often confined to mechanically stiff units in central Montana, where more extensive fracturing develops, and brecciation is more widespread.
2. The migration of CO_2 within these brittle features was most likely associated with the formation of breccia pipes and hydrothermal alteration. Such migration pathways would have been enhanced by CO_2 effervescence ("boiling") before a loss of thermodynamic temperature or pressure ceased movement of brine solutions.
3. Breccias in central and south central Montana have had a strong hydrothermal influence, as evidenced by strongly negative $\delta^{18}O$ values compared to the standard (VPDB). This isotopic depletion often indicates higher temperatures during vein- and matrix- filling stages due to decreased oxygen fractionation between water and calcite (Budai and Wiltschko, 1987).
4. Different isotopic compositions within vein fill material indicate that fluid flow has occurred in more than one episode. Some of the possible sources of fluids related to veining include Cretaceous marine or meteoric water, connate fluids, and basinal brines (Budai and Wiltchko, 1987).

Multi-spectral imaging for detecting CO_2 leaks

J. Shaw

Multispectral imagers used to detect plant stress caused by CO_2 leaking from underground.

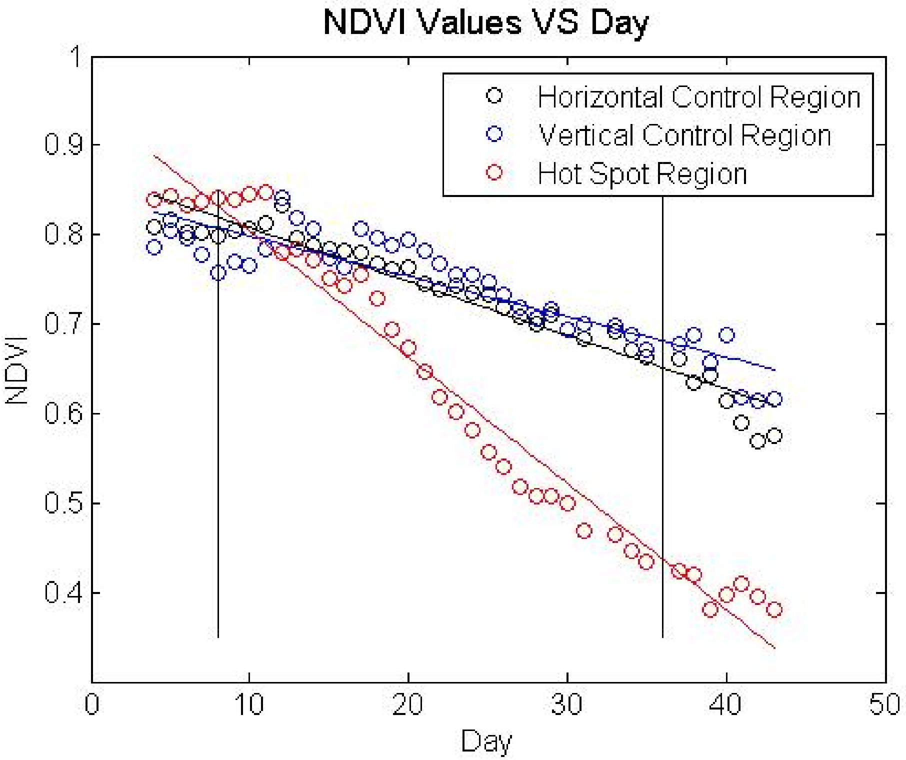

Time-series plot showing that the CO_2-affected plant health decays faster over time than the control region. This plot shows Normalized Difference Vegetation Index (NDVI), found from NIR and red reflectances as (NIR-red)/(NIR+red)

Tethered balloon multispectral imaging at ZERT

J. Shaw

Compact, ultra-low-cost multi-spectral imager designed for deployment on tethered balloon.

Tethered balloon multispectral imaging at ZERT

J. Shaw

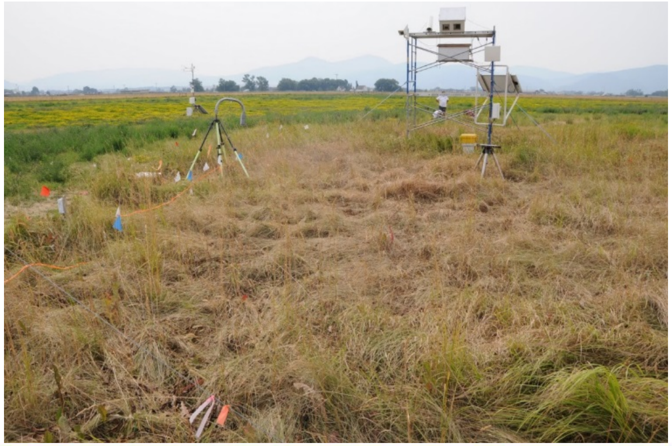

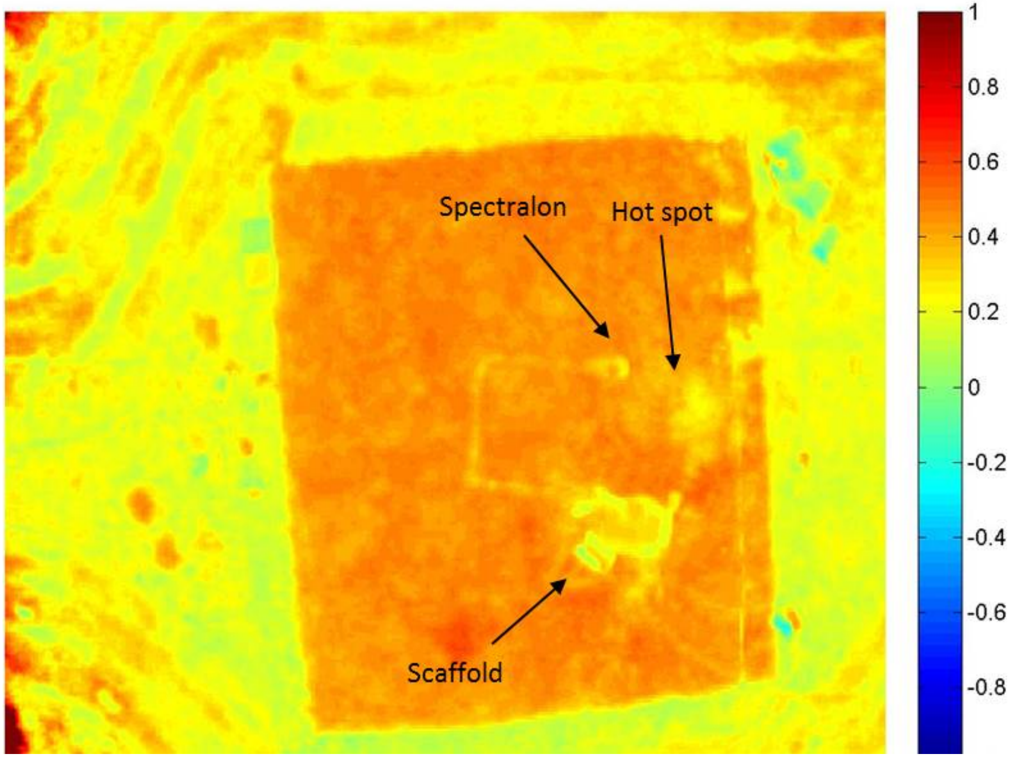

NDVI image from the balloon-borne imager tethered 50 m above the ZERT site on July 5, 2012, before the CO_2 gas release.

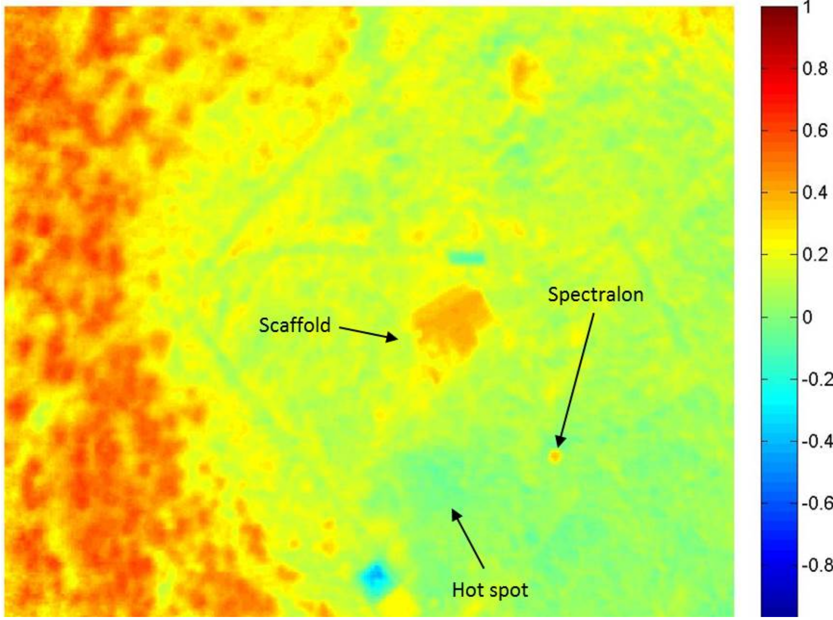

NDVI image from the balloon-borne imager tethered 50 m above the ZERT site on August 10, 2012, at the end of the CO_2 gas release.

Comparison of multispectral imaging at ZERT

J. Shaw

Scaffolding, more expensive instrument

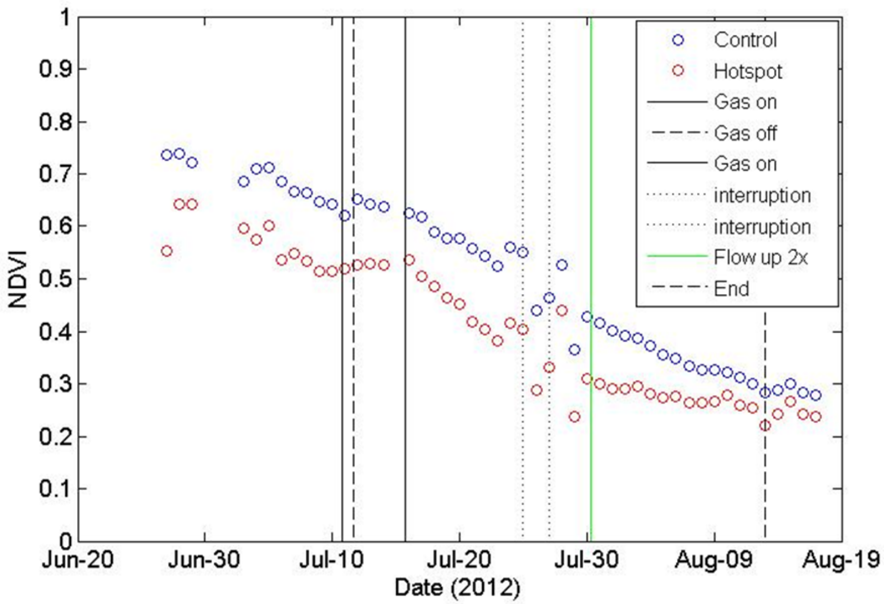

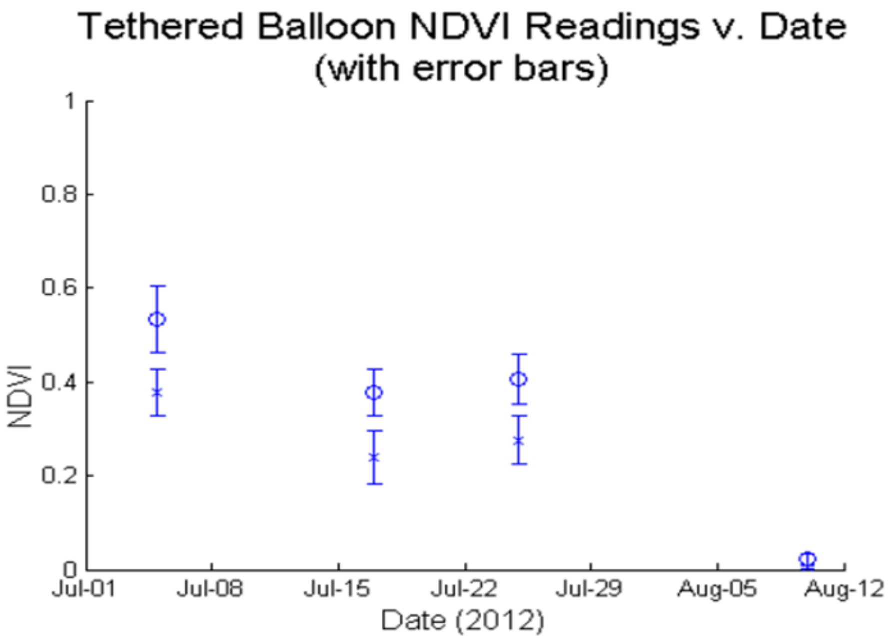

Long-wave thermal vegetation imaging to detect CO_2

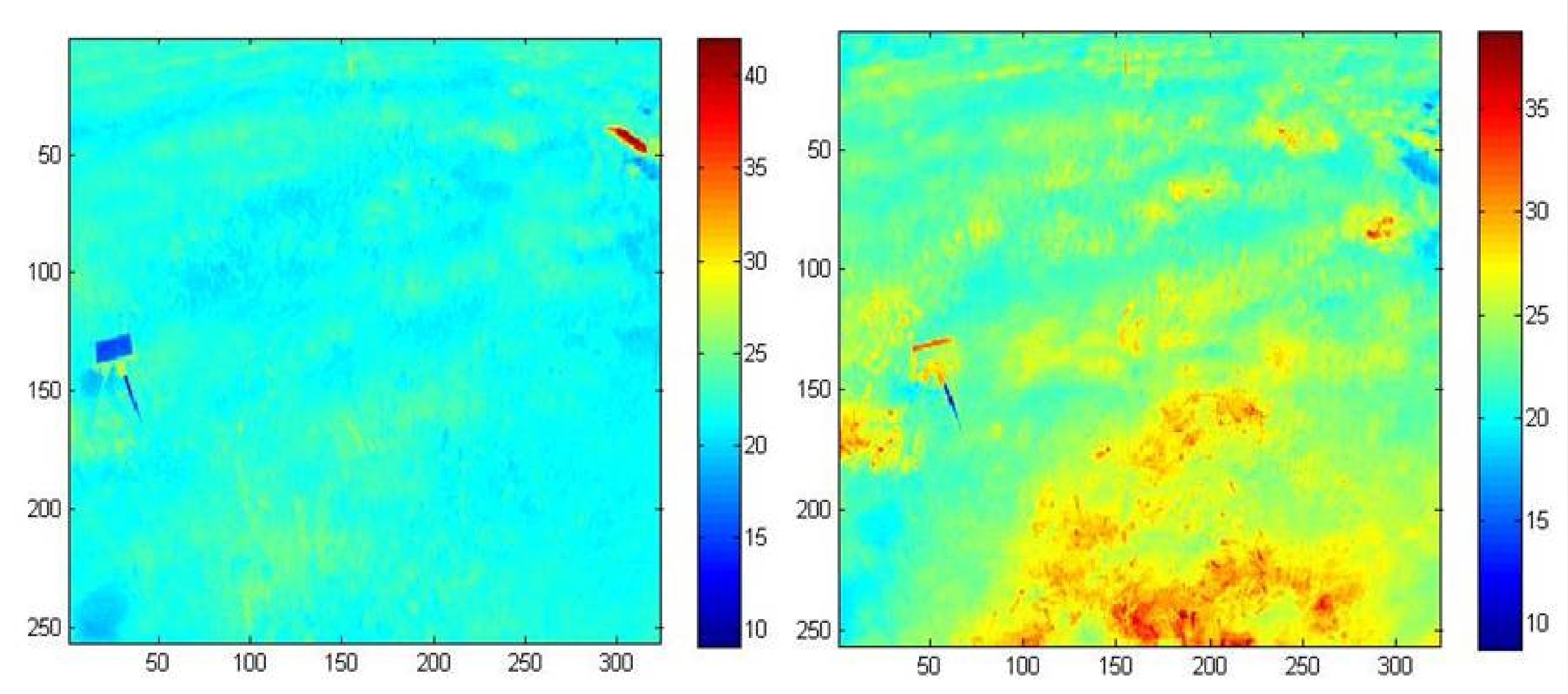

Thermal images (°C) for 10 AM, 7/13/2011 (left) and 10 AM, 8/10/2011 (right). The right-hand image shows that the plant temperatures are much higher with high CO_2 flux (the -1,0) hot spot is just outside the lower-right corner).

ZERT Zero Emissions Research and Technology

MONTANA STATE UNIVERSITY

Long-wave thermal vegetation imaging to detect CO_2

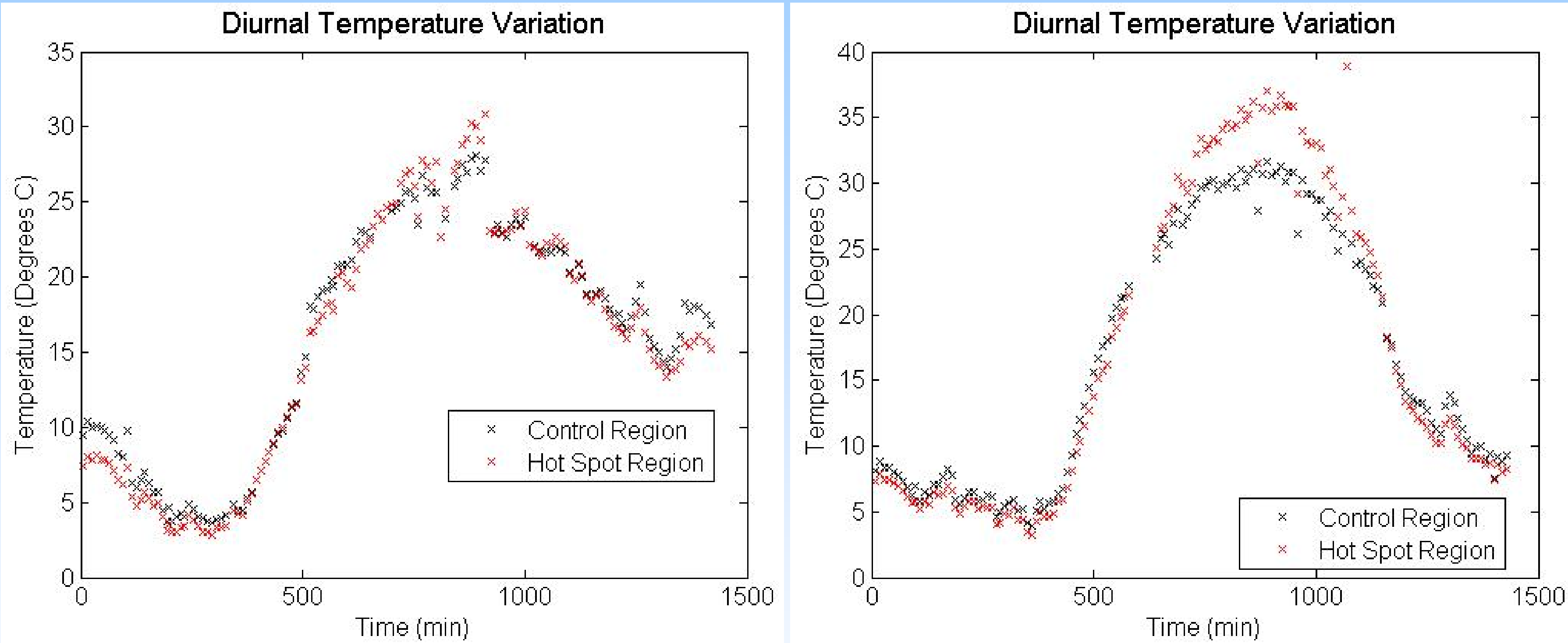

LWIR vegetation brightness temperature plotted vs time for a 24-hour period from midnight to midnight: (left) start of the release, and (right) end of the release.

Inline Fiber Sensor

K. Repasky

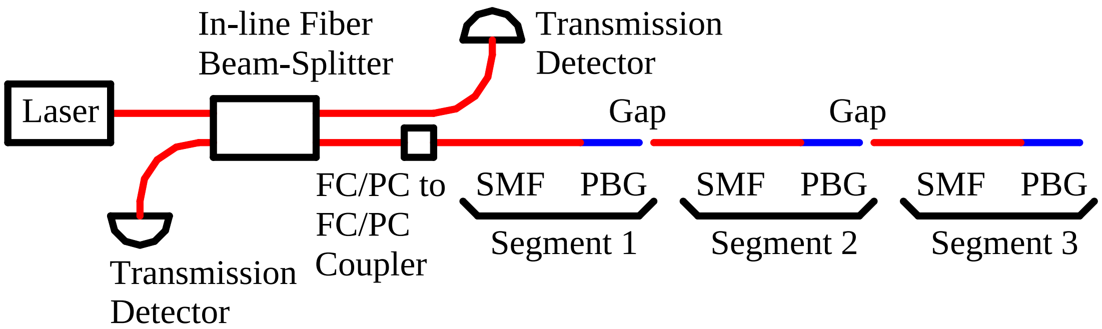

The inline fiber sensor uses a series of segmented photonic bandgap (PBG) fiber in series to for a inline fiber sensor array.

Each segment is addressed using time of flight of the laser pulse.

CO_2 diffuses into the PBG fiber to allow spectroscopic measurements of CO_2 concentration.

Challenge: PBG fiber is larger diameter than SMF and conventional splicing collapses hollow core

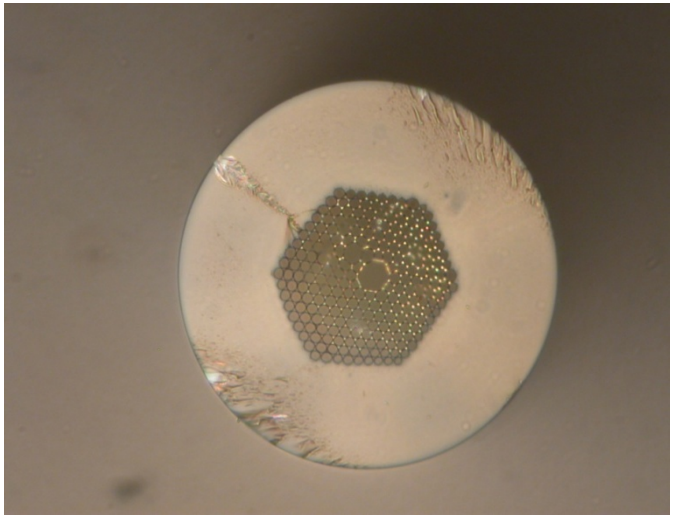

The PBG fiber allows interaction of the laser light and CO_2 in the hollow core.

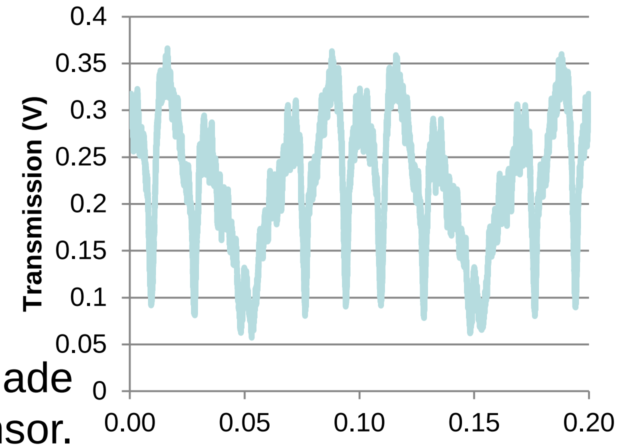

Initial un-normalized CO_2 measurements made using one segment of the inline fiber sensor.

Microfab V-Groove Coupler

K. Repasky

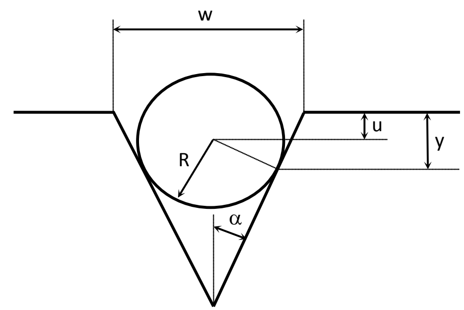

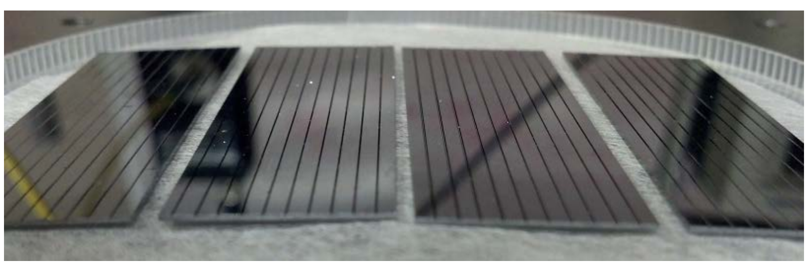

Diced silicon substrate containing the V-Groove structures.

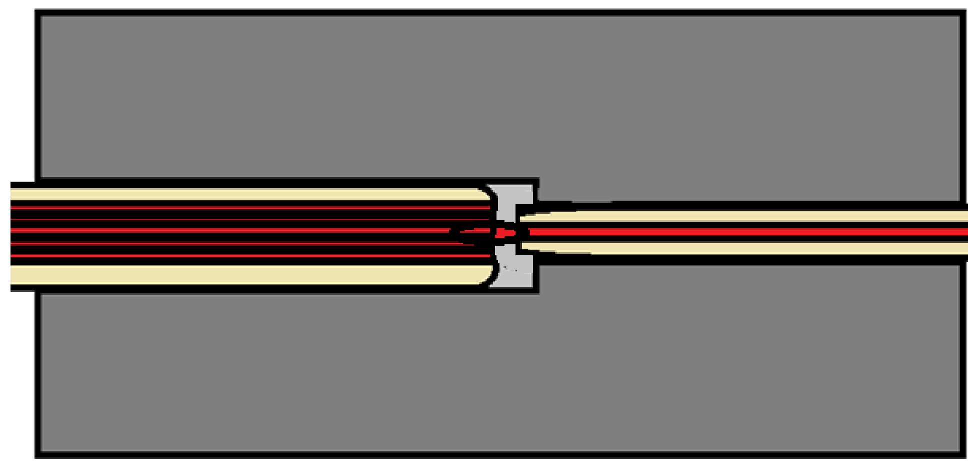

Microbially Induced Carbonate Precipitation (MICP)

Cunningham, Gerlach

+ pH and alkalinity (increase in OH^- and HCO_3^-) increase SATURATION STATE OF CALCITE

$CO(NH_2)_2 + H_2O \rightarrow NH_2COOH + NH_3$

$NH_2COOH + H_2O \rightarrow NH_3 + H_2CO_3$

$CO(NH_2)_2 + 2\ H_2O \rightarrow 2\ NH_3 + H_2CO_3$ (Urea hydrolysis)

$2NH_3 + 2H_2O \leftrightarrow 2NH_4^+ + 2OH^-$ (pH increase)

$H_2CO_3 + 2OH^- \leftrightarrow HCO_3^- + H_2O + OH^- \leftrightarrow CO_3^{2-} + 2\ H_2O$

$CO_3^{2-} + Ca^{2+} \leftrightarrow CaCO_3$ (carbonate precipitation)

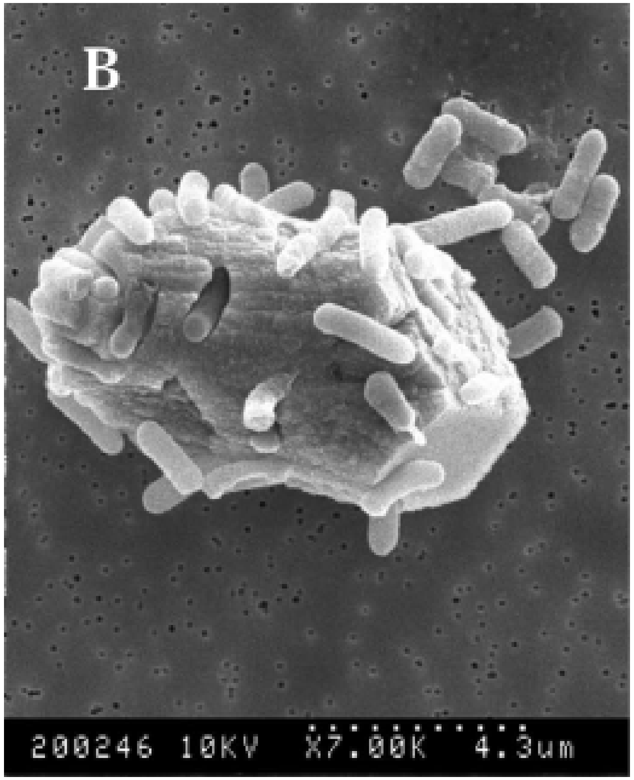

Model ureolytic organism: *Sporosarcina pasteurii*

Ureolysis is only one possible way to manipulate the saturation state of carbonates

Mitchell, AC and Ferris, FG (2006). *Geomicrobiology Journal* , 23, 213-226.

Mitchell, AC. and Ferris, FG. (2006) *Environmental Science and Technology, 40, 1008-1014.*

Mitchell, AC. and Ferris FG. (2005) *Geochimica Et Cosmochimica Acta, 69, 4199-4210.*

Calcite Precipitation Control

Cunningham, Gerlach

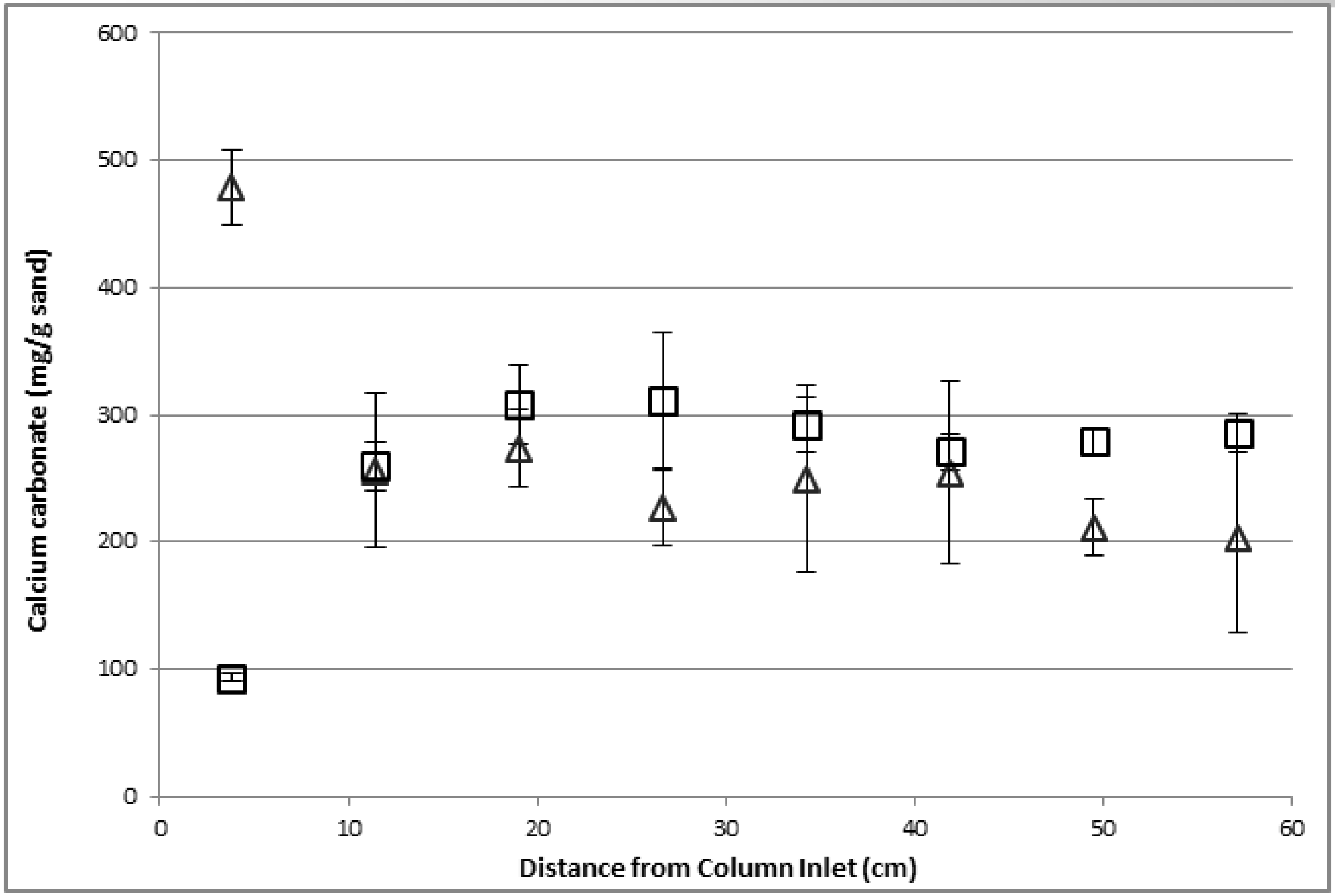

Improved distribution and prevented inlet plugging by adding "flushing" steps to displace calcium in the influent region

$CaCO_3$ concentration (mg) per gram of sand by ICP-MS in vertically positioned column experiments (ΔColumn #1; □Column #5, near-injection-point displacement strategy).

Bio-sealants in Mont Terri
Conducted by Montana State University

Permeability reduction due to biomineralization in one-inch diameter Opalinus shale core drilled from original shale sample, July 18, 2013

Core locations on the Opalinus shale sample

ZERT Zero Emissions Research and Technology

MONTANA STATE UNIVERSITY

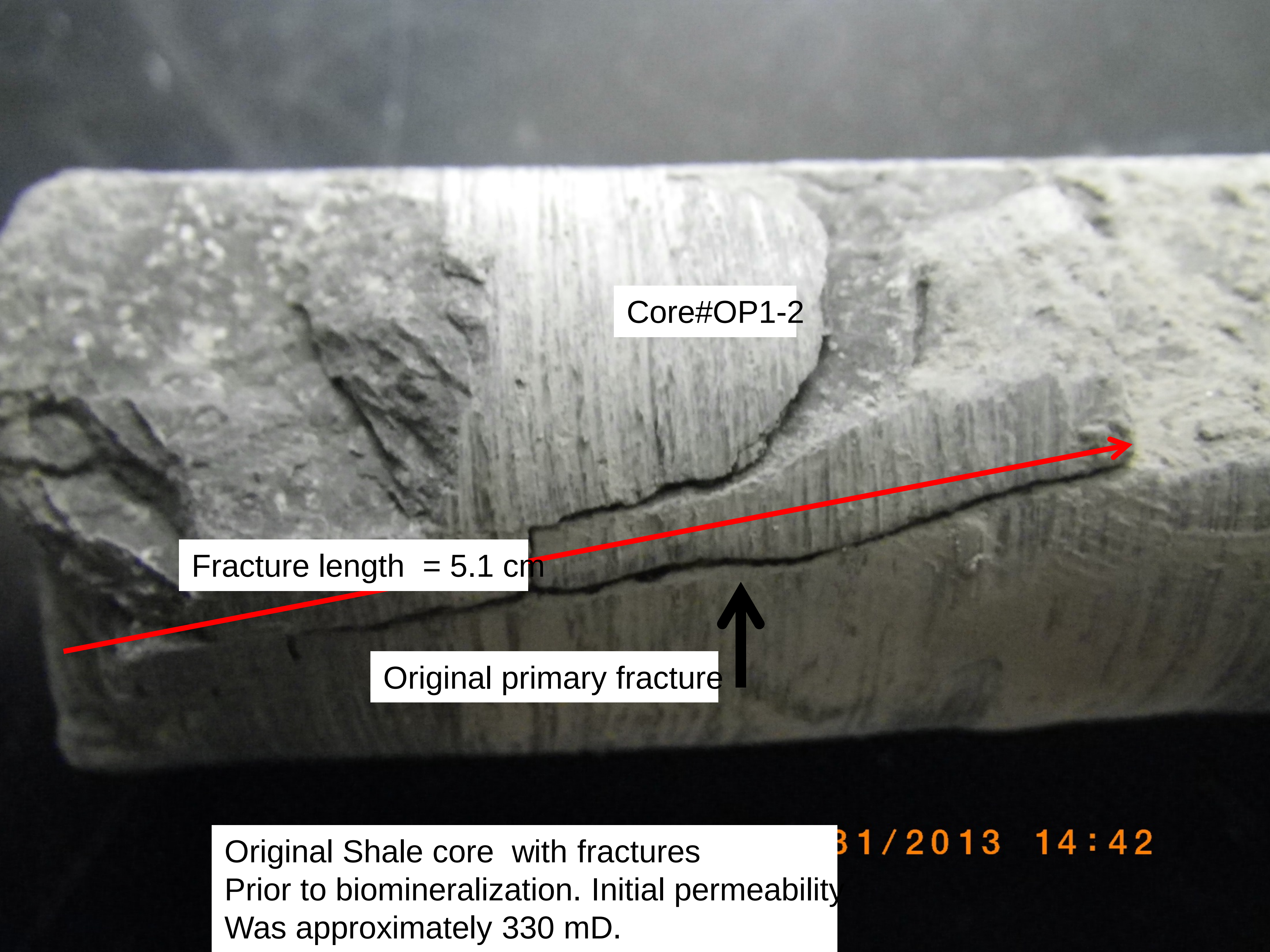

Original Shale core with fractures
Prior to biomineralization. Initial permeability
Was approximately 330 mD.

Simple ambient condition reactor for initial tests

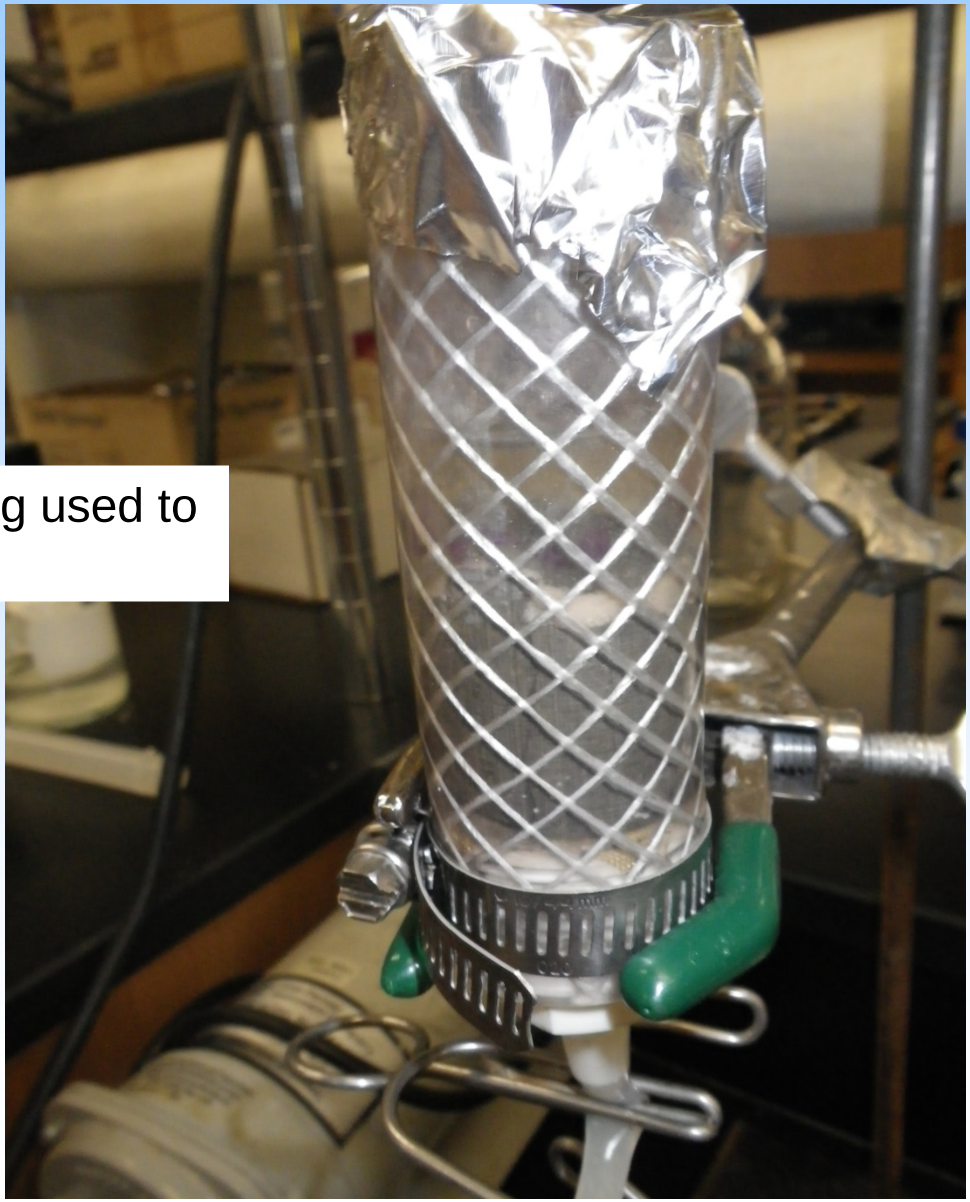

Braided PVC Tubing used to test shale cores

Checked progress when permeability reduced to 6.3 mD

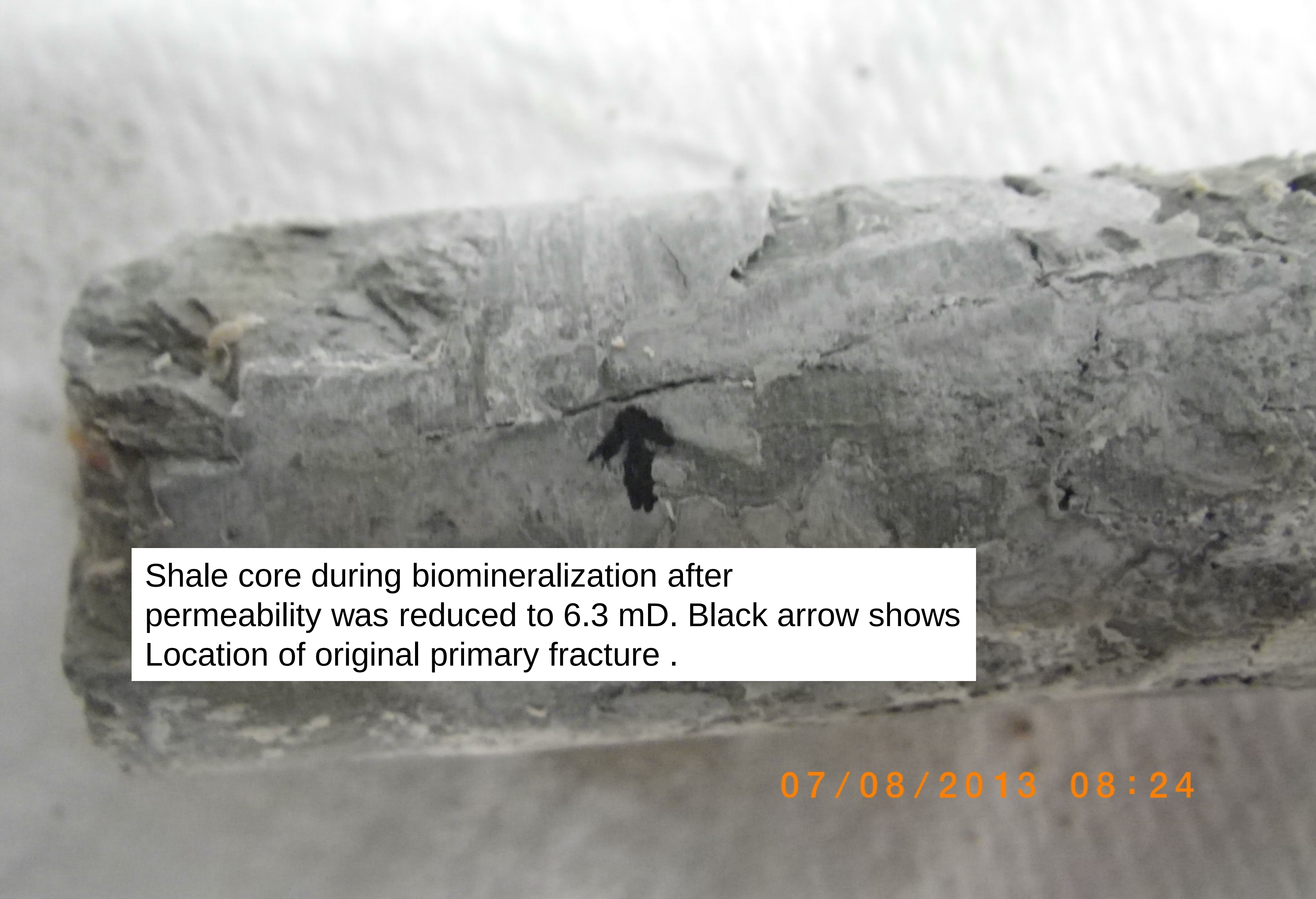

Shale core during biomineralization after permeability was reduced to 6.3 mD. Black arrow shows Location of original primary fracture .

Resumed biomineralization

- Re-inserted the core in new PCV tubing and resumed the biomineralization
- At the conclusion of this test we had lowered our flow rate to 0.305 mL per hour, which was the lowest possible setting on our syringe pump.
- At this point we observed a pressure drop of 16.1 psig and a permeability of 0.08 mD

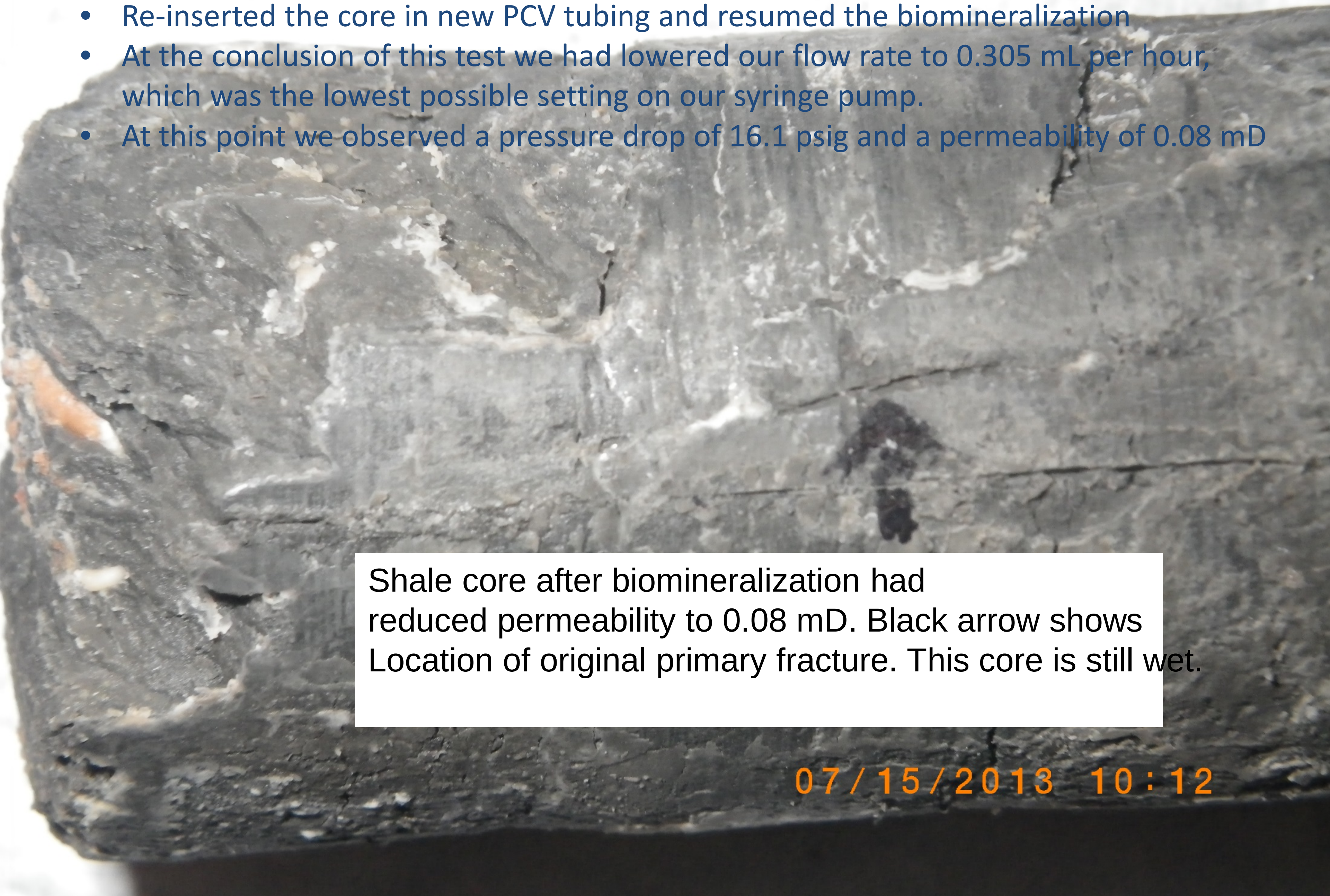

Shale core after biomineralization had reduced permeability to 0.08 mD. Black arrow shows Location of original primary fracture. This core is still wet.

ZERT Zero Emissions Research and Technology

MONTANA STATE UNIVERSITY

Sustainable microbial coal bed methane production

Methane can be formed through the biotransformation of organic matter (including coal and oil) by methane producing microorganisms (*Methanogens*).

By supplying appropriate nutrients to the coal & oil deposits microbial methane production can be enhanced and sustained over time

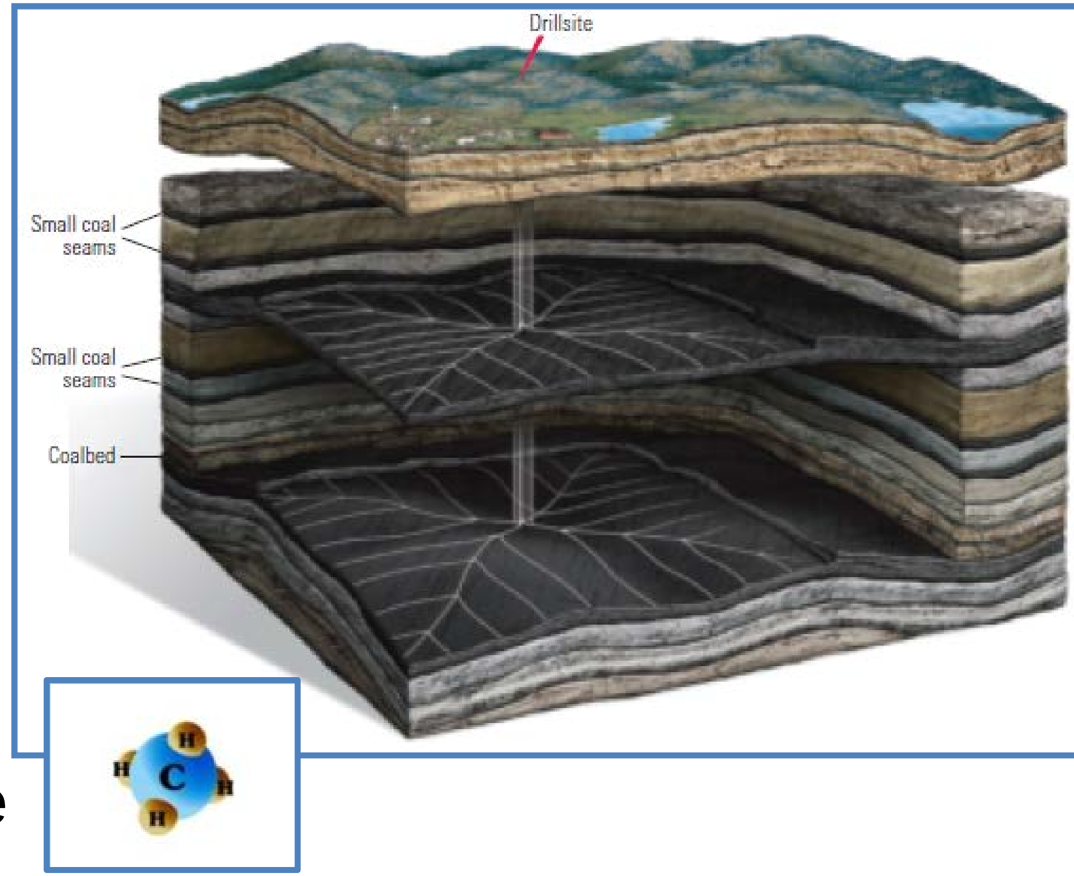

Novel Down-hole Microbial Sampler

(invented by Elliott Barnhart, ZERT-funded PhD student)

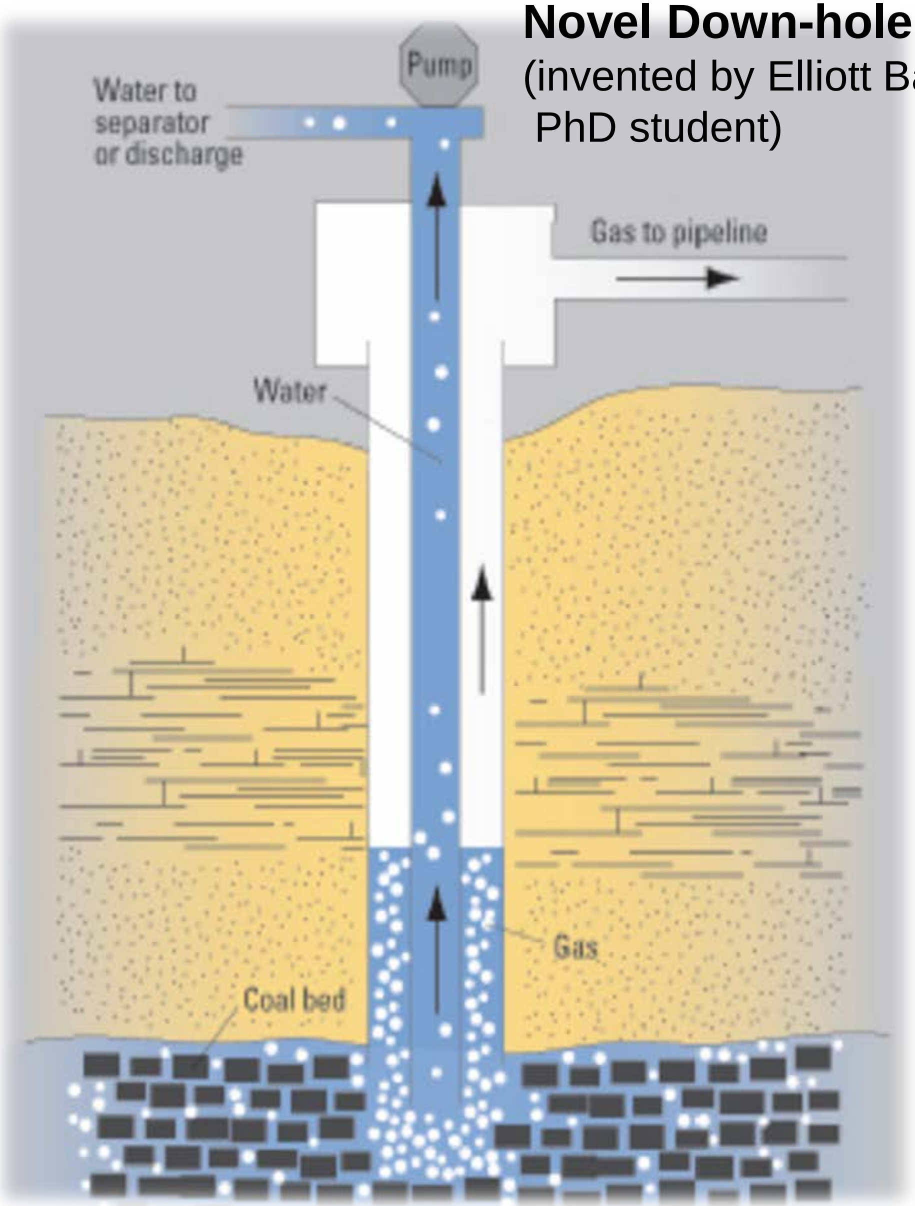

Novel down-hole microbial sampler.
The sampler is lowered to the
depth of the coal seam and opened
Thereby allowing indigenous
microbes to colonize the coal sample attached
To the bottom of the sampler. After several
months
The sampler is retrieved and the coal sample is
analyzed for microbial presence and abundance

Sampling Powder River coal beds, October 2011

Conducted by USGS with MSU student participation

Lab Results:
Biostimulation of methane production from coal

- Batch systems with native PRB microbes
- Increased methane with algae extract

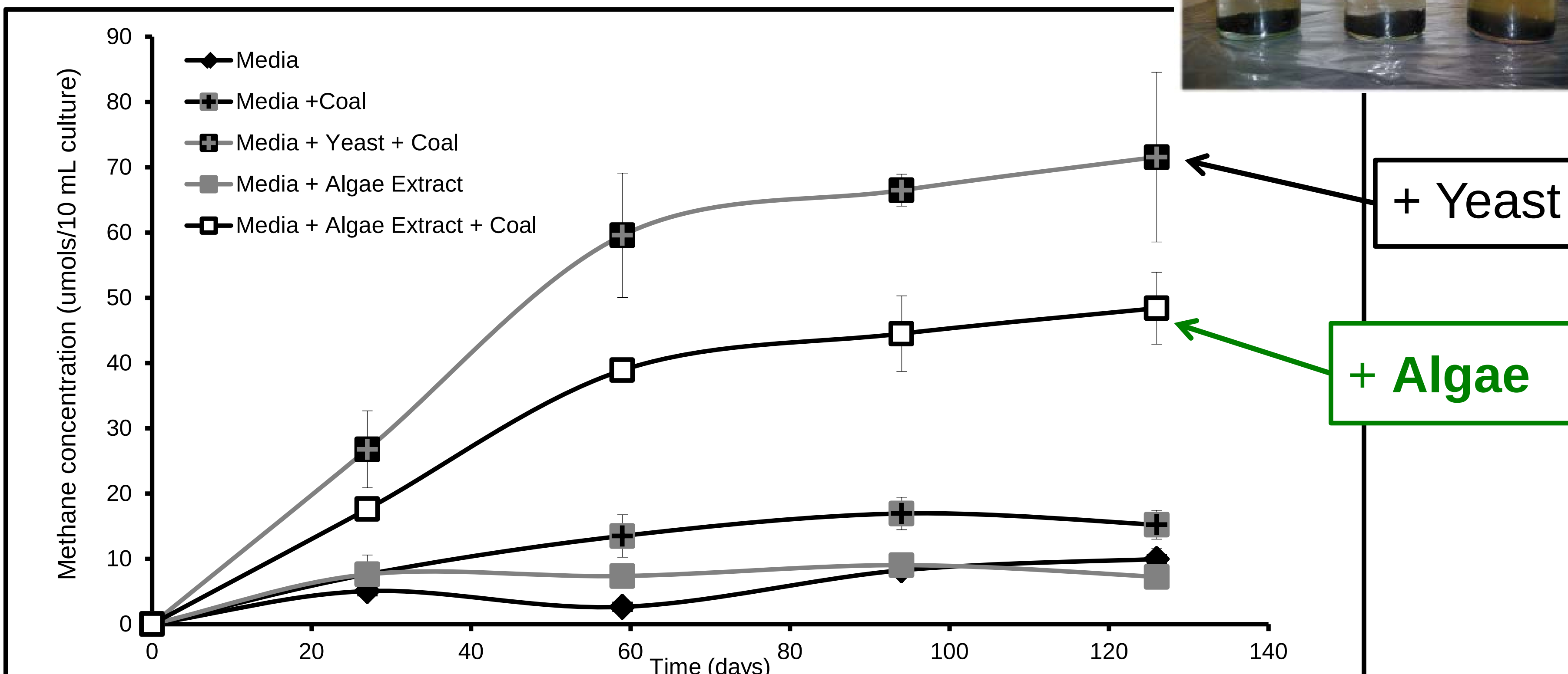

Barnhart *et al.* in prep

2013 CBM Fiel

- Biogenic methane production in the Powder River Basin is high (dark red circles) in the recharge zone then decreases as ground water flow moves North East.
  (Bates *et al.* (2011) Chem Geol 284:45-6)

- Using a novel down-hole microbial sampler Elliott Barnhart (PhD student) was able to identify DNA sequences related to algae and cyanobacteria. Samples were taken from well WR 53-A.

- Analysis of this data strongly suggests that the biogenic methane production in this Powder River Basin recharge zone is being stimulated and sustained by phototrophic micro organisms (algae) which infiltrate in coal beds from surface recharge.

- These results are being prepared for submission to *Applied and Environmental Microbiology* by Elliott Barnhart and other ZERT scientists

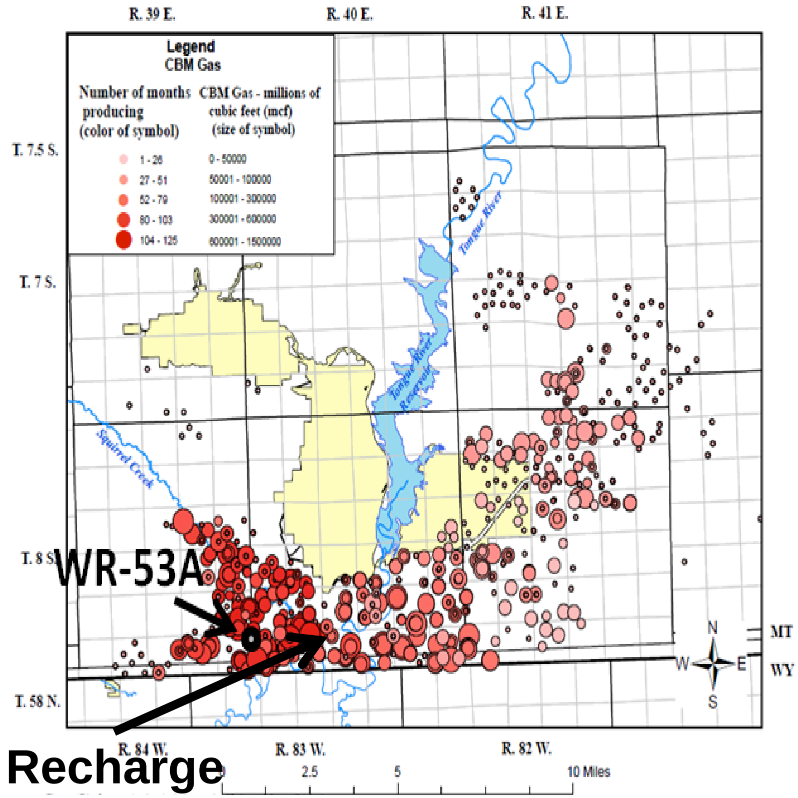

Meredith *et al.* (2011) MBMG 600.

(Dark red circles indicate more productive wells)

MONTANA STATE UNIVERSITY

Fields, Cunningham

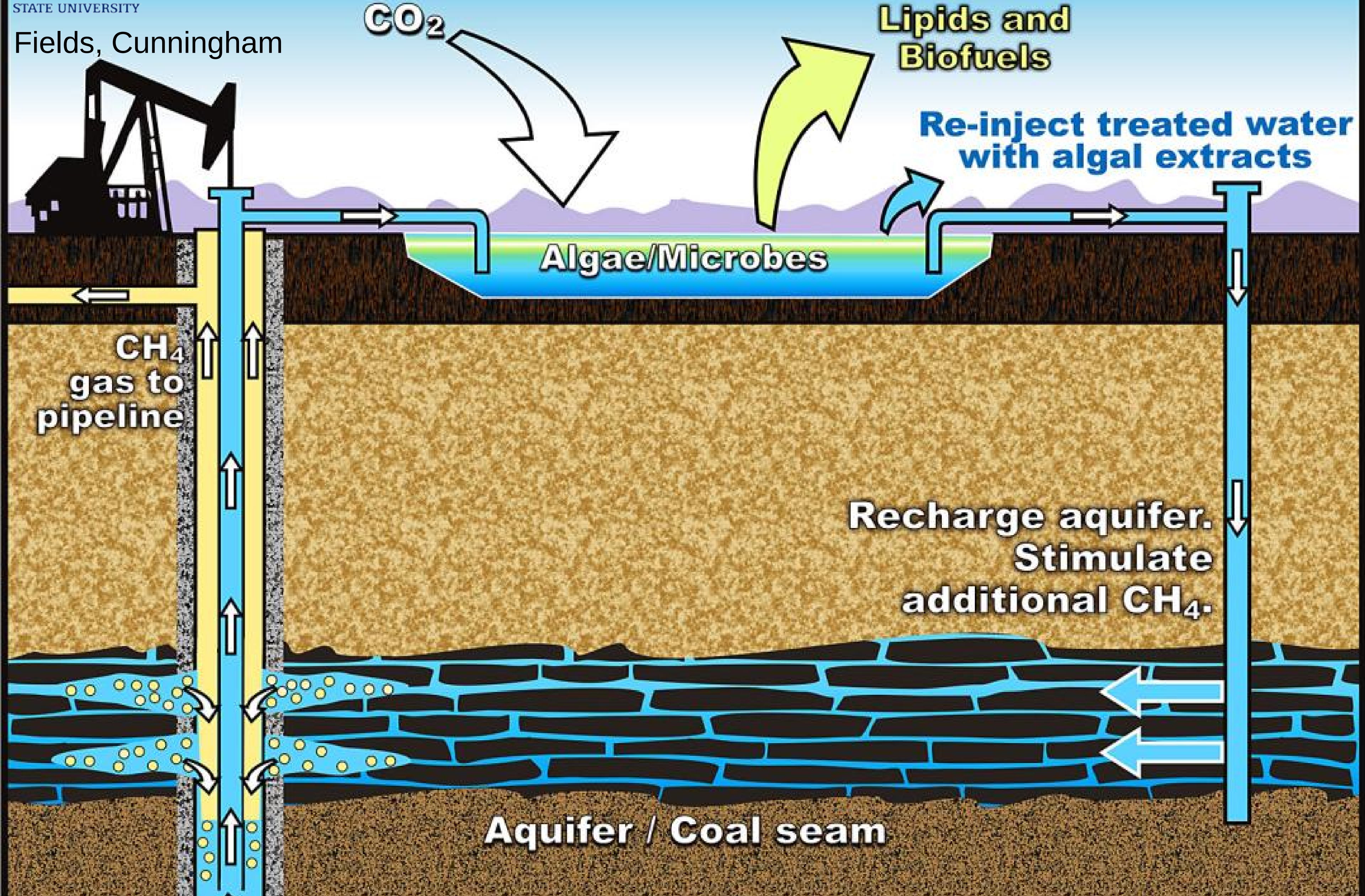

Accomplishments to Date

- Modified two computational codes used for CO_2 simulations
- Studied multiple analogs to inform risk assessment
- Developed and performed initial field tests on three prototype moderate area near surface detection technologies
- Performed studies to deepen understanding of capillary trapping mechanism
- Hosted other academic institutions, gov. agencies and private sector entities in field experiment

Summary

- Multiple computational codes have been improved
- Near surface detection technologies have been tested
- Analogs are providing important information to understanding of risk

Appendix

– These slides will not be discussed during the presentation, but are mandatory

Organization Chart

Multi-Institutional Management Structure

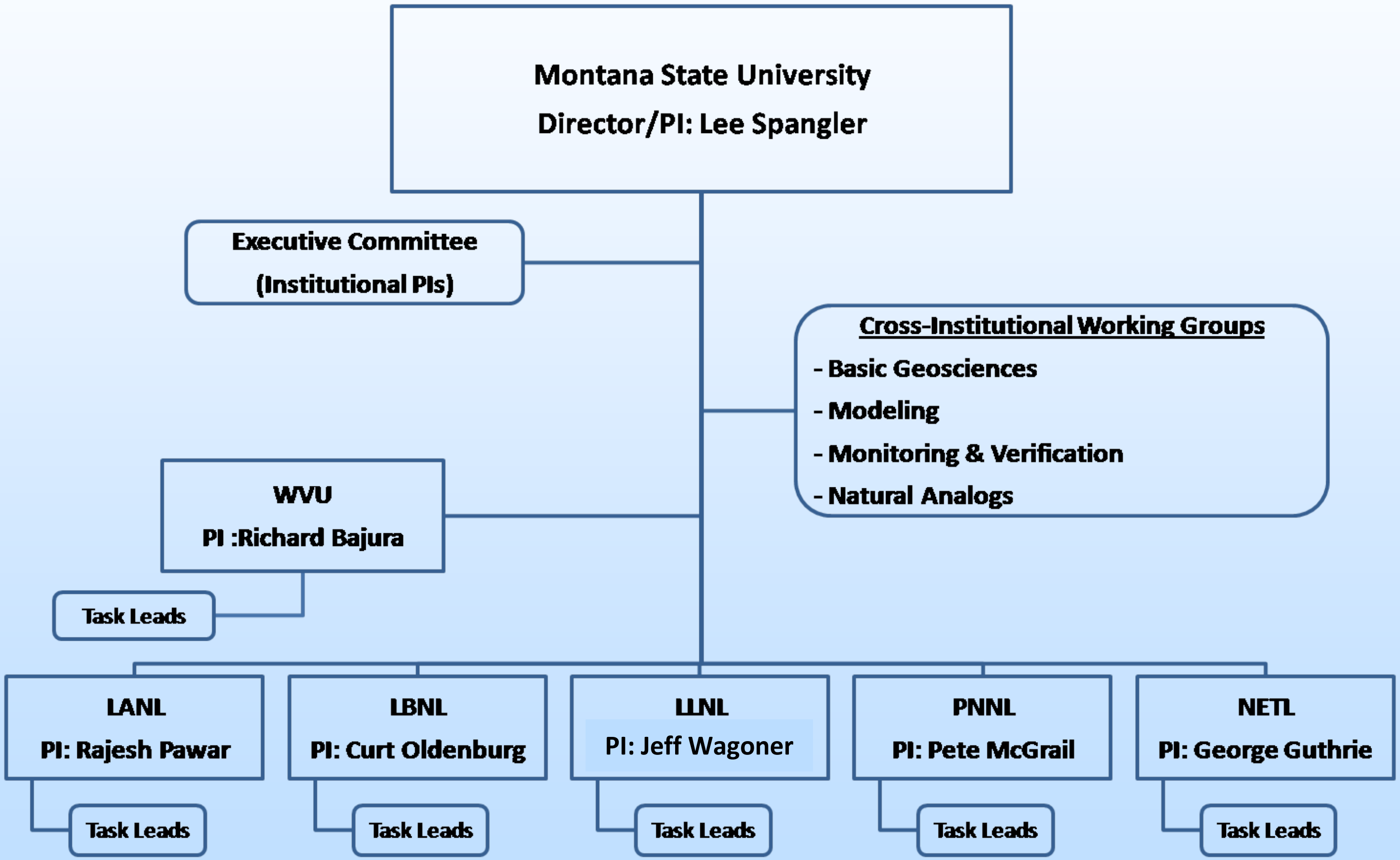

Organization Chart

MSU Internal Management Structure

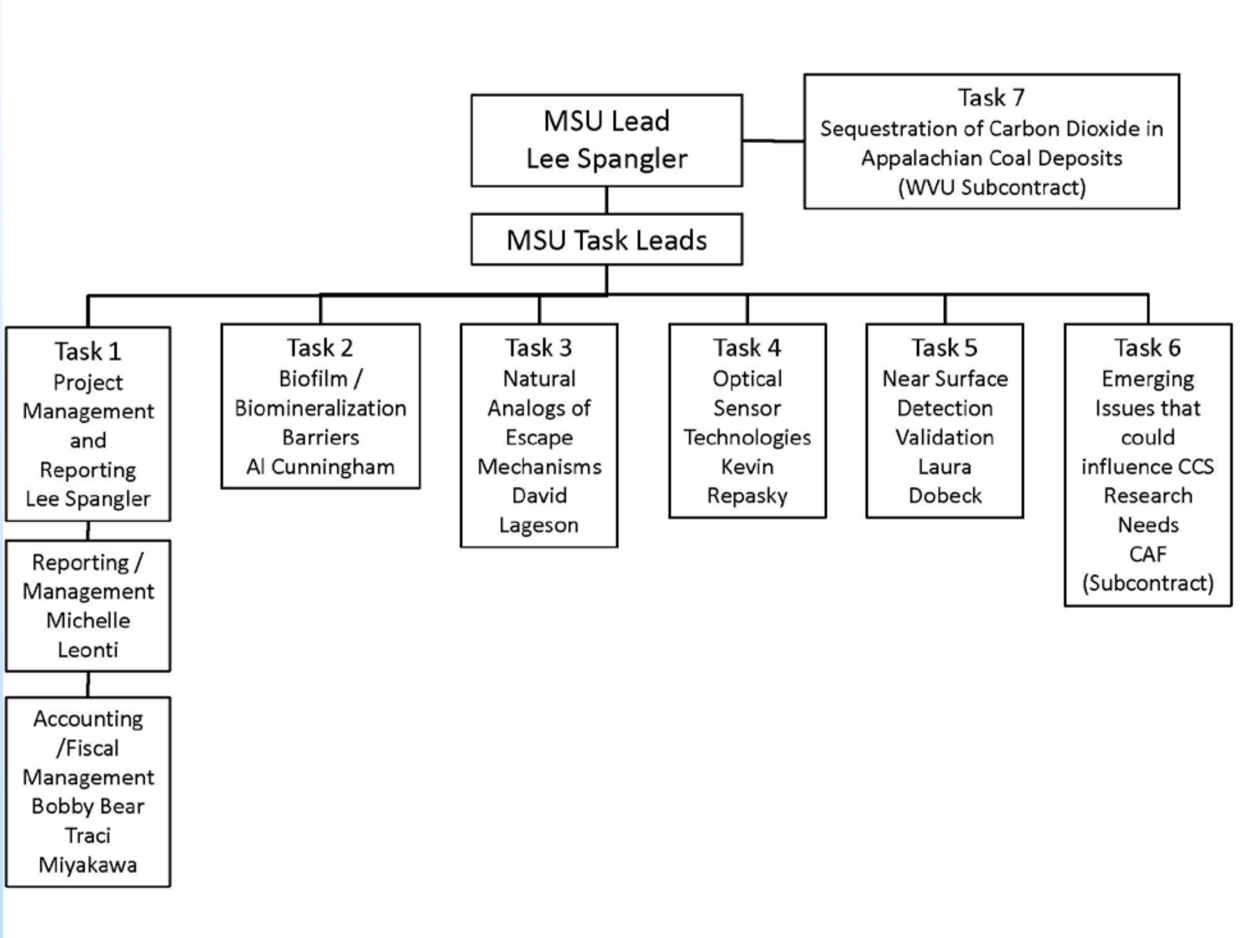

Gantt Chart

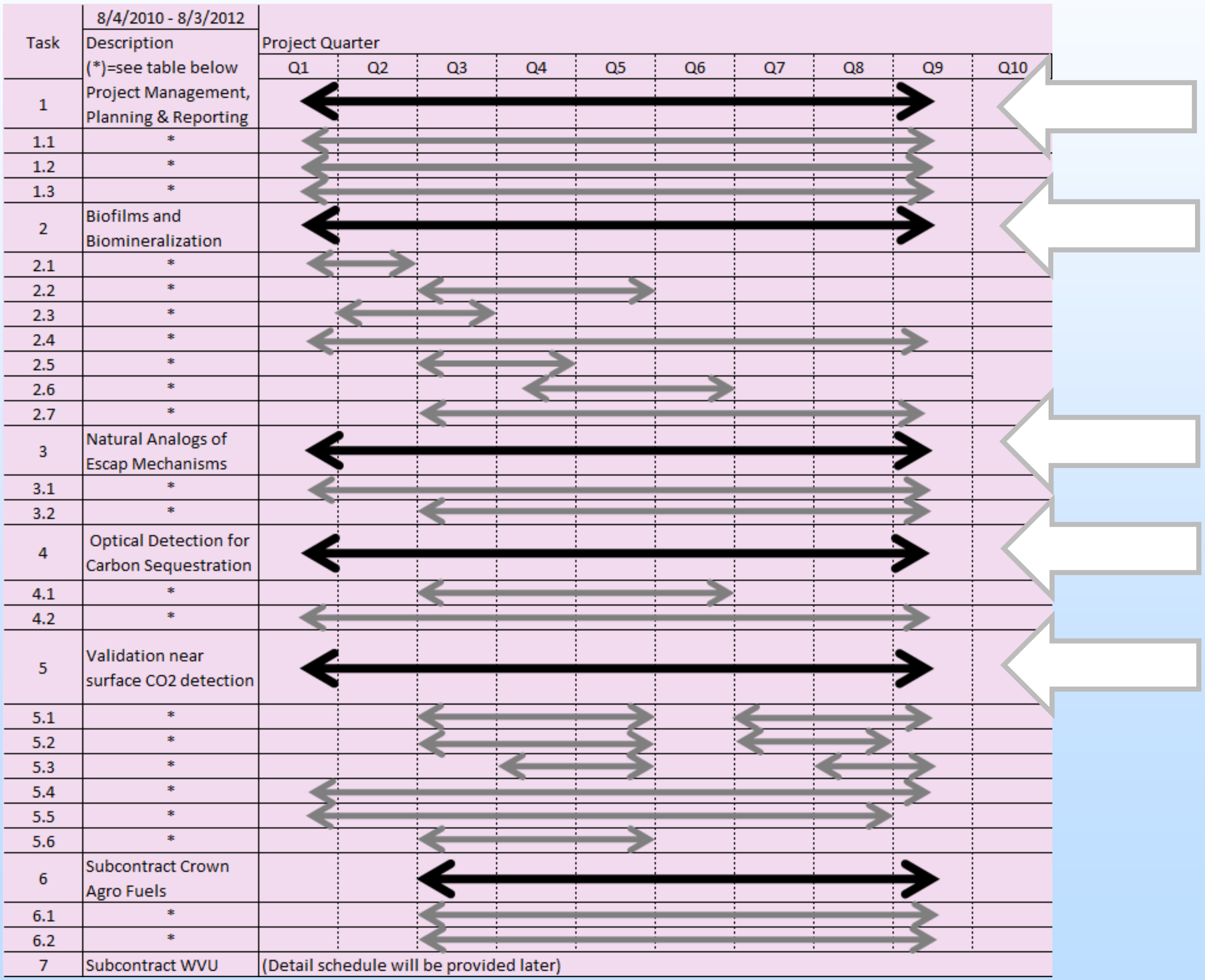

The tasks are continued in the no-cost extension awarded in August 2012.

Gantt Chart

Cont.

Task 1.0 – Project Management, Planning, and Reporting
Subtask 1.1 Project Management
Subtask 1.2 Project Reporting
Subtask 1.3 Presentations and Briefings
Task 2.0 – Biofilms and Biomineralization
Subtask 2.1 Conduct experiments on CO_2 biomineralization deposits on flat coupons and in porous media bead packs.
Subtask 2.2 Develop method to control deposition rate of biomineralized calcium carbonate with distance along a porous media flow path.
Subtask 2.3 Optimize biomineralization of isotopically labeled CO2 carbon under variable head space pressure.
Subtask 2.4 Evaluate the potential for coalbed mediated CO2 sequestration.
Subtask 2.5 Construct a system capable of flowing supercritical fluids through the bore of the magnet of the NMR spectrometer.
Subtask 2.6 Evaluate transport phenomena for brine and supercritical CO2 using magnetic resonance techniques.
Subtask 2.7 Evaluate transport phenomena for brine and supercritical CO2 in a bead pack or other model porous media.
Task 3.0 – Natural Analogs of Escape Mechanisms
Subtask 3.1 Leakage versus Confinement Associated with Subsurface Migration of Natural CO_2 across Faults and Fracture Networks
Subtask 3.2 Ancient Hydrothermal Plumes as a Natural Analog of Hydrofracing Caprocks and Geochemical Healing Mechanisms
Task 4.0 – Optical Detection for Carbon Sequestration Site Monitoring
Subtask 4.1 Underground Fiber Optic Sensors
Subtask 4.2 UltraCompact Thermal Infrared Imagers
Task 5.0 – Validation of Nearsurface CO2 Detection Techniques and Transport Models at Experimental Field Site.
Subtask 5.1 Seasonal Site Preparation
Subtask 5.2 Coordinate experimental season with ZERT team.
Subtask 5.3 Collect data in support of ZERT research project goals.
Subtask 5.4 Investigate opportunities for greater involvement outside of the ZERT team.
Subtask 5.5 Support optical remote sensing group
Subtask 5.6 Support pollen capture of tracers experiments:
Task 6.0 – Tracking Emerging Issues That Could Influence CCS Research Needs
Subtask 6.1 Provide information to government at the state, federal and international levels.
Subtask 6.2 Provide information to NGOs, industry groups, and professional groups relevant to CCS.
Task 7.0 – Sequestration of Carbon Dioxide in Appalachian Coal Deposits (WVU Subcontract)
(Detailed Task and Subtask descriptions will be provided at a later date.)

Bibliography

1. Barnhart, E., Bowen, D., Ramsay, B., Cunningham, A.B. and Fields, M., Coal-Associated Bacterial and Archaeal Populations: Coal-Dependant Increased Bacterial Diversity. International Journal of Coal Geology, 2013. 115(2013): p. 64-70.
2. Fang, Y., Nguyen, K., Carroll, M., Xu, Y., Yabusaki, T., Scheibe, A. and Bonneville, A., Development of a coupled thermo-hydro-mechanical model in discontinuous media for carbon sequestration. Int. J. Rock Mech. Min. Sci., 2013. 62(September 2013): p. 138-147.
3. Kneafsey, T., Silin, D. and Ajo-Franklin, J., Supercritical CO2 flow through a layered silica sand/calcite sand system: Experiment and modified Maximal Inscribed Spheres analysis,. International Journal of Greenhouse Gas Control, 2013. 14: p. 141-150.
4. Lauchnor, E., Schultz, L., Bugni, S., Mitchell, A., Cunningham, A. and Gerlach, R., Bacterially induced calcium carbonate precipitation and strontium co-precipitation in a porous media flow system. Environmental Science & Technology Journal, 2013. 47(3): p. 1557-1564.
5. Mitchell, A., Phillips, A., Schultz, L., Parks, S., Spangler, L., Cunningham, A. and Gerlach, R., Microbial CaCO3 mineral formation and stability in a simulated high pressure saline aquifer with supercritical CO2. International Journal of Greenhouse Gas Control, 2013. 15: p. 86-96.

Bibliography

Cont.

6. Phillips, A., Gerlach, R., Lauchnor, E., Cunningham, A. and Spangler, L., Engineered applications of ureolytic biomineralization: a review Biofouling, 2013. 29(6): p. 715-733.
7. Phillips, Lauchnor, E., Eldring, J., Esposito, R., Mitchell, A., Gerlach, R., Cunningham, A.B. and Spangler, L., Potential CO2 Leakage Reduction through Biofilm-Induced Calcium Carbonate Precipitation Environmental Science & Technology Journal, 2013. 47(1): p. 142-149.
8. Amonette, J.E., Barr, J.L., Erikson, R.L., Dobeck, L. and Shaw, J.A., Measurement of Advective Soil Gas Flux: Results of Field and Laboratory Experiments with CO2. Environmental Earth Sciences, 2012. Published online: February 2013.
9. Bonneville, A., Dermond, J., Strickland, M., Sweeney, M., Sullivan, E.C., Heggy, E. and Normand, J., Monitoring Surface Deformation Associated with an Aquifer Storage and Recovery (ASR) Site In Pendleton, OR, as an Analog for Subsurface CO2 Sequestration. Water Resources Research, 2012. Submitted.
10. Cunningham, A.B., Lauchnor, E., Eldring, J., Esposito, R., Mitchell, A., Gerlach, R., Phillips, Ebibo, A. and Spangler, L., Abandoned Well CO2 Leakage Mitigation Using Biologically Induced Mineralization: Current Progress and Future Directions. Greenhouse Gases: Science and Technology, 2012. 3(1): p. 40-49.

Bibliography

Cont.

11. Ebigbo, A., Phillips, Gerlach, R., Helmig, R., Cunningham, A.B., Class, H. and Spangler, L., Darcy-Scale modeling of Microbially Induced Carbonate Material Precipitation In Sand Columns. Water Resources Research, 2012. 48(W07519)
12. Hogan, J.A., Shaw, J.A., Lawrence, R.L. and Larimer, R.L., A low-cost multi-spectral imager for detecting gas leaks indirectly from changes in vegetation reflectance. Appl. Opt., 2012. 51(4): p. A59-A66.
13. Hogan, J.A., Shaw, J.A., Lawrence, R.L., Lewicki, J.L., Dobeck, L. and Spangler, L., Detection of leaking CO2 gas with vegetation reflectances measured by a low-cost multispectral imager. IEEE J. Selected Topics Appl. Earth Obs. And Rem. Sens, 2012. 5(3): p. 699-706.
14. Johnson, J., Shaw, J.A., Lawrence, R.L., Nugent, P., Dobeck, L. and Spangler, L., Long-wave Infrared Imaging of Vegetation For Detecting Leaking CO2 Gas. Journal of Applied Remote Sensing. 2012. 6(063612).

Bibliography

Cont.

15. Keating, E., Hakala, Viswanathan, H.S., Carey, R., Pawar, R.J., Guthrie, G.D. and Fessenden, J., CO2 leakage impacts on shallow groundwater: field-scale reactive-transport simulations informed by Observations at a natural analog site. Applied Geochemistry, 2012. 30: p. 136-147.
16. Kihm, J., Kim, J.M., Wang, C. and Xu, T., Hydrogeochemical numerical simulation of impacts of mineralogical compositions and convective fluid flow on trapping mechanisms and efficiency of carbon dioxide injected into deep saline sandstone aquifers. Journal of Geophysical Research, 2012. 117(B06204).
17. Lageson, D.R., Larsen, M.C., Lynn, H.B. and Treadway, W.A., Applications Of Google Earth Pro to Fracture and Fault Studies of Laramide Anticlines in the Rocky Mountain Foreland Whitmeyer, S.J., Bailey, J.E., De Paor, D.G., and Ornduff, T., eds., Google Earth and Virtual Visualizations in Geoscience Education and Research, 2012. In Review(492a.): p. 1-12.
18. Lewicki, J.L. and Hilley, G.E., Eddy covariance network design for mapping and quantification of surface CO2 leakage fluxes. International Journal of Greenhouse Gas Control, 2012. 7: p. 137-144.

Bibliography

Cont.

19. Viswanathan, H.S., Z., D., C., L., Keating, E., Hakala, K., S., Zheng, L. and Pawar, R.J., Developing a robust geochemical and reactive transport model to evaluate possible sources of arsenic at the CO2 sequestration natural analog site in Chimayo, New Mexico. International Journal of Greenhouse Gas Control, 2012. 10: p. 199-214.
20. White, M.D., Bacon, D.H., McGrail, B.P., Watson, T.L., White, S.K. and Zhang, G., STOMP: Subsurface Transport Over Multiple Phases: STOMP-CO2 and -CO2e Guide. PNNL-21268, 2012.
21. Windisch, C.F., Maupin, J.G.D. and McGrail, B.P., Soret Effect Study on High- Pressure CO2-Water Solutions Using UV-Raman Spectroscopy and a Concentric-Tube Optical Cell. Technical Report PNNL-21156, 2012.
22. Windisch, C.F., Maupin, J.G.D. and McGrail, B.P., Ultraviolet (UV) Raman Spectroscopy Study of the Soret Effect in High-Pressure CO2-Water Solutions. Applied Spectroscopy, 2012. 66(7): p. 731-739.
23. Zhou, X.B., Lakkaraju, V.R., Apple, M., Dobeck, L., Gullickson, K.S., Shaw, J.A., Cunningham, A.B., Wielopolski, L. and Spangler, L., Experimental observation of signature changes in bulk soil electrical conductivity in response to engineered surface CO2 leakage. International Journal of Greenhouse Gas Control, 2012. 7: p. 20-29.

Bibliography

Cont.

24. Cunningham, A.B., Gerlach, R., Spangler, L., Mitchell, A., Parks, S. and Phillips, A., Reducing the risk of well bore leakage of CO2 using engineered biomineralization barriers. Energy Procedia, 2011. 4: p. 5178-5185.
25. Pruess, K., Integrated Modeling of CO2 Storage and Leakage Scenarios Including Transitions between Super- and Sub-Critical Conditions, and Phase Change between Liquid and Gaseous CO2. Greenhouse Gases: Science and Technology, 2011. 1(3): 237-247.
26. Xu, T., Spycher, N., Sonnenthal, N., Zhang, G., Zheng, L. and Pruess, K., TOUGHREACT Version 2.0: A Simulator for Subsurface Reactive Transport under Non-isothermal Multiphase Flow Conditions,. Computers & Geosciences, 2011. 37(6): p. 763-774.
28. Xu, T., Zheng, L. and Tian, H., Reactive Transport Modeling for CO2 Geological Sequestration. Petroleum and Science and Engineering, 2011. 78: p. 765-777.
29. Zhang, W., Xu, T. and Li, Y., Modeling of fate and transport of coinjection of H2S with CO2 in deep saline formations. Journal of Geophysical Research-Solid Earth, 2011. 116(B02202): p. 13.

Bibliography

Cont.

30. Keating, E., Hakala, J.A., Viswanathan, H.S., Capo, R., Stewart, B., Gardiner, J., Guthrie, G.D., Casey, J.W. and Fessenden, J., The challenge of predicting groundwater quality impacts in a CO2 leakage scenario: Results from field, laboratory, and modeling studies at a natural analog site in New Mexico, U.S.A. Energy Procedia, 2011. 4: p. 3239-3245.
31. Krupa, K.M., Cantrell, K.J. and McGrail, B.P., Thermodynamic Data for Geochemical Modeling of Carbonate Reactions Associated with CO2 Sequestration –Literature Review. PNNL-19766, 2010.
32. Silin, D., Tomutsa, L., Benson, S.M. and Patzek, T., Microtomography and Pore Scale Modeling of Two-Phase Fluid Distribution. Transport in Porous Media, 2010: p. 1-21.

Hyperspectral Aerial Detection

K. Repasky

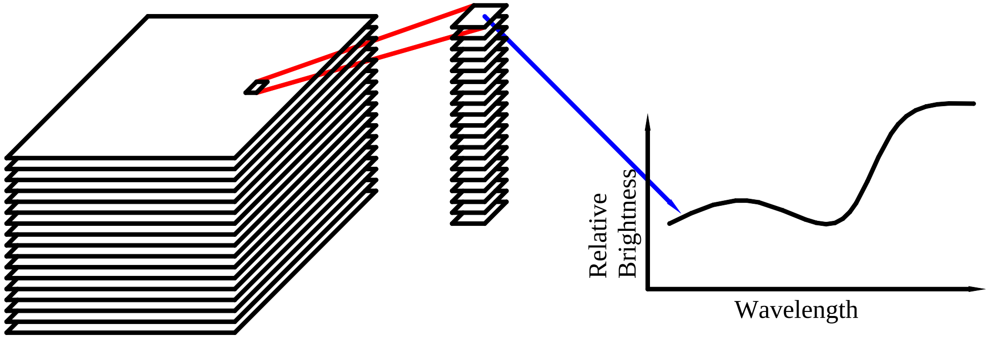

Image simultaneously acquired in many narrow adjacent wavelength bands

For each spatial pixel, a brightness value is defined for each wavelength band

For one spatial pixel, the brightness value for each wavelength band is plotted as a function of wavelength to create a reflectance spectrum

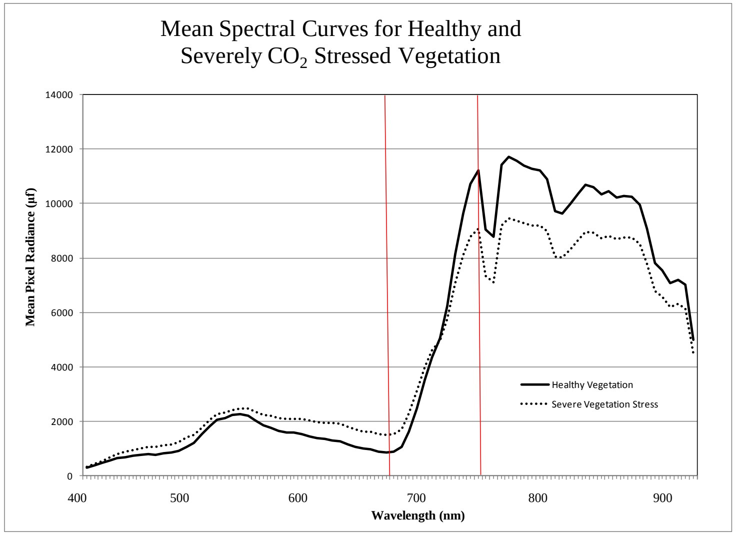

For each pixel in the image, a reflectance spectra – amount of light reflected as a function of wavelength -- is generated

Stressed vegetation can be detected be detected using subtle changes in the reflectance spectra resulting from plant physiology

Hyperspectral Aerial Detection

K. Repasky

Flight based hyperspectral imaging allows large area monitoring needed for carbons sequestration sites

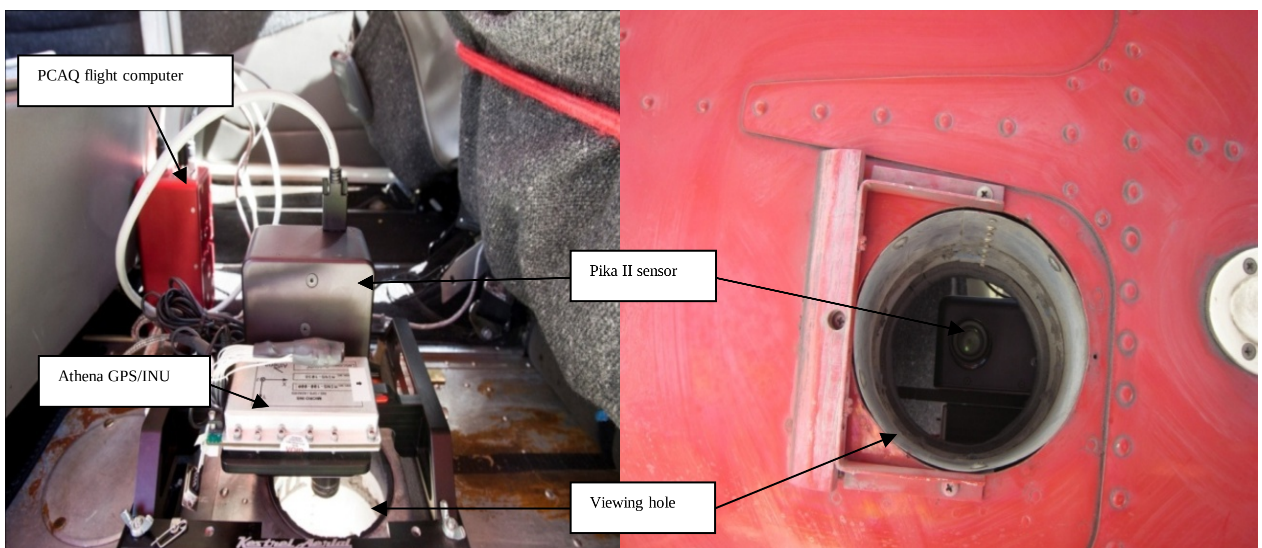

Hyperspectral Aerial Detection at the ZERT Site

K. Repasky

Aerial view of the ZERT field site

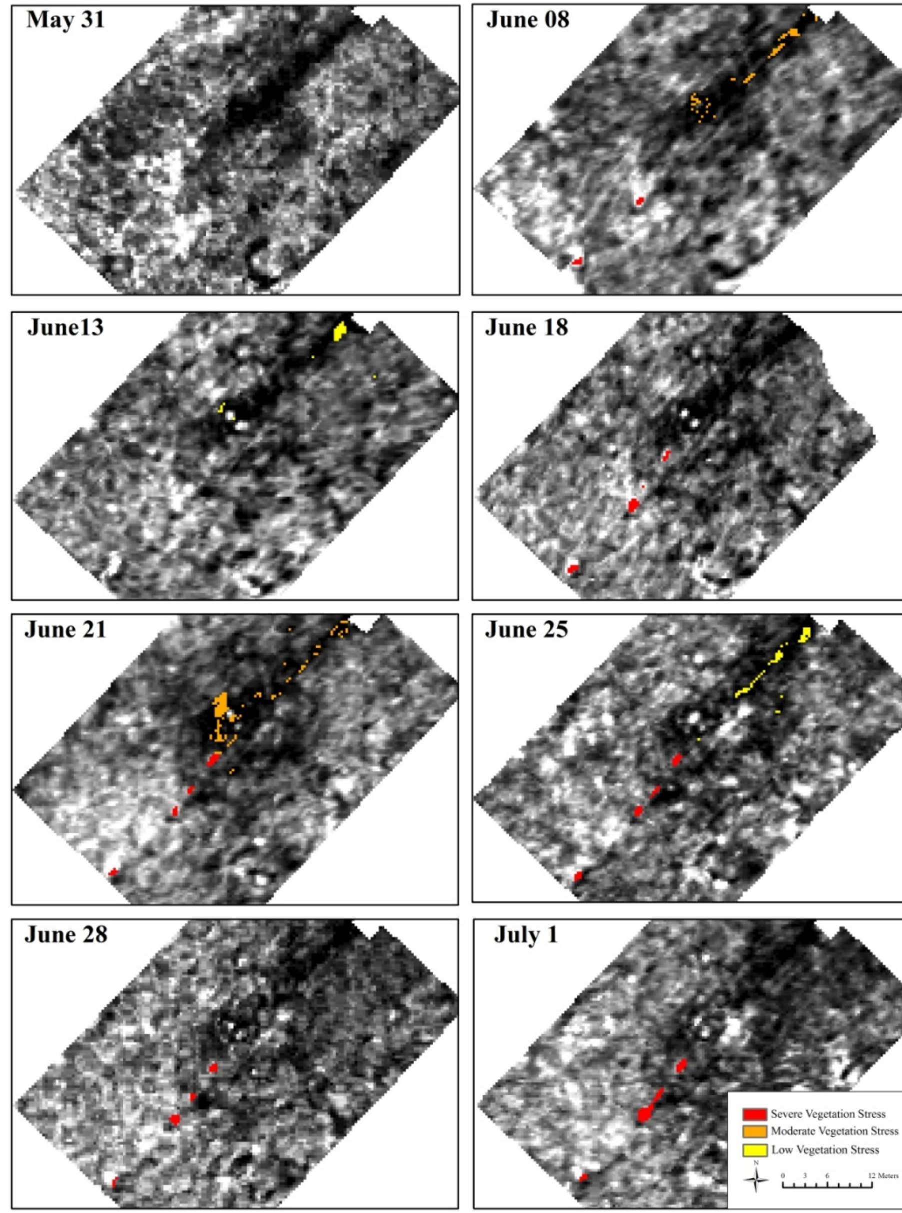

Evolution of the vegetation stress over the course of a month long sub-surface release at the ZERT field site.

The stress vegetation correlates with chamber measurements of carbon dioxide providing a validation of this method.